A Thesis

On

VIBRATION BASED ANALYSIS OF DEFECTS IN ROTATING SHAFTS

Submitted in the partial fulfilment of requirement for

the award of degree

MASTER OF ENGINEERING

In

PRODUCTION AND INDUSTRIAL ENGINEERING

By

Rajdeep Singh

Regn. No.-800982020

Under the supervision of

Dr. V. P. Agrawal
Visiting Professor

Dr. P. K . Kankar
Assistant Professor

DEPARTMENT OF MECHANICAL ENGINEERING

THAPAR UNIVERSITY, PATIALA (PUNJAB)

July-2011

Dedicated To My Loving Parents

CERTIFICATE

This is to certify that the work done in this thesis report titled **"VIBRATION BASED ANALYSIS OF DEFECTS IN ROTATING SHAFTS"** submitted in partial fulfilment of requirement for the award of Master of Engineering degree in Production and Industrial Engineering in the Mechanical Department of Thapar University, Patiala is an authentic record of work carried out by me under the guidance of Dr. V. P. Agrawal, Visiting Professor and Dr. P. K. Kankar, Assistant Professor, Mechanical Engineering Department, Thapar University, Patiala.

The matter embodied in this report has not been submitted in part or full to any other university or institute for the award of any degree.

Rajdeep Singh

(Rajdeep Singh)

This is to certify that above declaration made by the student concerned is correct to the best of my knowledge & belief.

Dr. V.P. Agrawal
Visiting Professor
Deptt. of mechanical Engg.
Thapar University, Patiala

05.07.11

Dr. P. K. Kankar
Assistant Professor
Deptt. of mechanical Engg.
Thapar University, Patiala

Countersigned by:

Dr. Ajay Batish
Professor & HOD
Deptt. of Mechanical Engg.
Thapar University, Patiala

Dr. S.K. Mohapatra
Dean,
Acadamic Affairs
Thapar University, Patiala

ACKNOWLEDGEMENT

I am highly grateful to the authorities of Thapar University, Patiala for providing this opportunity to carry out the thesis work.

I express my deep gratitude and respects to my guides ***Dr. V. P. Agrawal and Dr. P.K . Kankar*** *for their keen interest and valuable guidance, strong motivation and constant encouragement during the course of the work. I thank them for their great patience, constructive criticism and myriad useful suggestions apart from invaluable guidance to me.*

I thank our head of department ***Dr. Ajay Batish****, whose excellent leadership and administration made this research project very convenient in term of required stuff and nice working condition. I am extremely thankful to member of distinguished faculty.*

The non-teaching staff ***Mr. Rajender, Mr. Sukhbir, Mr. Satwinder Singh, Mr. Charanjit Singh, Mr. Rajinder,*** *deserve special thanks for their help during the period of this work.*

I am also thankful to other faculty members and all the workshop staff of Mechanical Department, Thapar University, Patiala for their support.

Some friends were never too busy to give me a hand whenever they were needed. No word acknowledge the support I received from ***Sorav Sharma, Karanpreet Singh, Ramandeep Singh, Ankush Kumar, Dhiman Johns, Manjot Singh,*** *for their valorous help and co-operation.*

Last but not the least, I would like to thank my ***parents*** *and my* ***sister*** *for always being there when I needed them most and for their moral support that kept my spirit up during the endeavour.*

Rajdeep singh

ABSTRACT

The present study aims at the analysis of vibration responses of a horizontal rotor supported on ball bearings and to develop a fault diagnosis system for rotor systems. The sources of vibration in the rotor are the presence of different types of defects, which are cracks in the shaft, bent shaft and misalignment of shafts. These defects are considered with different severity level and their effect on vibration response has been analyzed using response surface methodology.

This study gives designers a diagnostic tool for predicting the trends of vibration conditions in a rotor bearing system for healthy and defective shaft conditions. The devised tool has capability of quantifying the amplitude of vibration based on severity of defects in shafts. In such cases, severe vibration has occurred in the system only due to either large slant crack or due to high level of shaft speed. With the features available in the devised diagnostic tool, the proposed model can be used for design, predictive maintenance of a rotor bearing system and also for condition monitoring of high speed rotating machines.

TABLE OF CONTENTS

LIST OF FIGURES

LIST OF TABLES

NOMENCLATURE

ADC = Amplitude Deviation Curve

AFT = Alternate Frequency Time domain

AMB = Active Magnetic Bearing

CWT = Continuous Wavelet Transforms

dFRFs = directional frequency response functions

dS = directional spectrum

EMD = Empirical Mode Decomposition

FFT = Fast Fourier Transform

HHT = Hilbert–Huang Transform

ODS = Operational Deflection Shape

RMS = Root Mean Square

RSM = Response Surface Methodology

SDC = Slope Deviation Curve

SERR = Strain Energy Release Rate

VC = Varying Compliance Frequency

WFE = Wavelet Finite Element

X = rotational frequency of shaft

x_0 = factors on which response variable depend

y_0 = response variable of interest

β = imbalance orientation angle

ω_c = critical frequency of shaft

ω_{cage} = cage frequency of bearing

ω_T = torsional excitation frequency

Chapter 1
INTRODUCTION

Shafts are the components which are subjected to the hardest conditions in high performance rotating equipments used in the process and utility plants like high speed compressors, steam and gas turbines, generators and pumps etc. Although when shafts are operated in different type of conditions then serious defects can appear, but these are much suspected to fatigue cracks because of the rapidly fluctuating nature of bending stresses. Because of manufacturing flaws or cyclic loading, cracks frequently appear in rotating shaft, other defects in shafts include bent shaft, misalignment etc. A defect on shaft can be diagnosed by many methods, e.g., ultrasonic detection, acoustic emission, vibration analysis. When shaft rotates then due to defect the vibrational response of the rotating shaft will more or less change. By using the additional vibration extracted from the shaft response due to defect, an on-line condition monitoring system for defect detection might be developed for rotor systems.

1.1 SOURCES OF VIBRATION IN THE ROTATING SHAFTS

1.1.1 Shaft Cracks

Cracks are defined as the unwilled discontinuities or separations in the shaft material. Based on the geometry cracks can be classified as follows: (Sabnavis et al., 2004)

(a) *Transverse Cracks*

The cracks which are perpendicular to the axis of rotor are called transverse cracks. These are most common among all the cracks and most serious, because these reduce the cross- section of the shaft.

(b) *Longitudinal Cracks*

The cracks parallel to the axis of the shaft are called longitudinal cracks.

(c) *Slant Cracks*

The cracks which are at an angle to the axis of the shaft are called slant cracks. These have similar effect on the rotor as that of transverse cracks, but the effect of these cracks on the

vibrations is less as compared to the transverse cracks.

(d) *Breathing Cracks*

The cracks which open up when the material having this crack is subjected to tensile stress and vice versa are called breathing cracks. The breathing of the crack results in the non-linearties in the vibrational behavior of the rotor. These cracks breathe when rotor speed is slow and radial forces are large.

(e) *Gaping Cracks*

Cracks that always remain open are called gaping cracks. These are also called notches.

(f) *Surface Cracks*

The cracks which are on the surface of the shaft are called surface cracks. These can easily be detected by dye-penetrate or visual inspection.

(g) *Sub-Surface Cracks*

The cracks which cannot be seen on the surface are called sub-surface cracks. These can be detected by radiography, ultrasonic magnetic particle and shaft voltage drop. These have less effect on the vibrational behavior of the rotor than that of surface cracks.

1.1.2 Unbalanced Shaft

Mass unbalance is the most prominent problem of a rotor system that may cause the entire machine to vibrate excessively. This may cause excessive wear in bearings, bushings, gears, and exhaust systems substantially and reduce their service life. When rotation begins, the unbalance exerts centrifugal force which tends to vibrate the rotor and its supporting structure. Centrifugal force increases proportionally to the square of the increase in speed.

1.1.3 Bend in the Shaft

When bent shaft rotates it produces vibrations which also cause damage to the bearings, Coupling (if it is connected to another shaft through coupling), and the structure on which it is mounted.

1.1.4 Misalignment of Shafts

When the two shafts are coupled together with the help of coupling then there can be a misalignment between them, which on rotating cause vibrations. There are two types of the misalignments.

(a) *Axial Misalignment*

When axes of the two coupled shafts are parallel but not coincident is called axial misalignment. This type of misalignment produces shear forces and bending moment on the coupled end of each shaft.

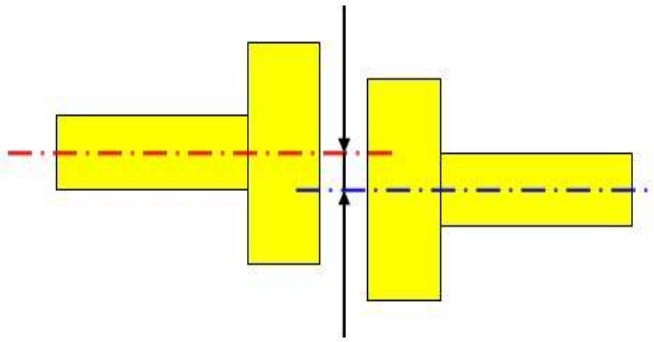

Figure 1.1 Axial Misalignment of Shafts (Jasmine, 2010)

(b) *Angular Misalignment*

Angular misalignment is the effective angle between the two shaft centerlines and is quantified by measuring the angle between the shaft centerlines as if they were extended till they intersect. This misalignment produces a bending moment on each shaft.

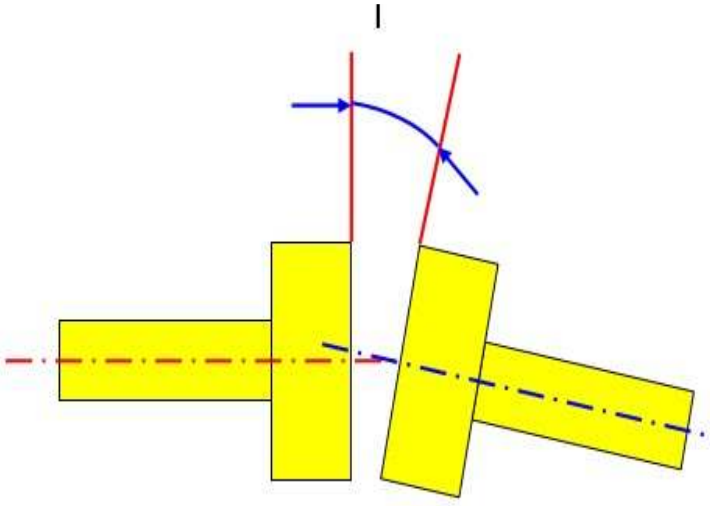

Figure 1.2 Angular Misalignment of Shafts (Jasmine, 2010)

1.2 FAILURE OF THE SHAFT

The shaft failure takes place in three steps (Sabnavis et al., 2004)

(a) *Crack Initiation*

In this stage tiny cracks or discontinuities appear. These are caused by sharp keyways; heavy shrink fit dents and the grooves, porosity and voids etc.

(b) *Crack Propagation*

When the rotor having the tiny crack is rotated or used then the small crack starts growing, this is called crack propagation. This occurs due to operating faults, thermal stresses, presence of residual stresses or welding heat affected zones.

(c) *Failure*

This stage comes when the crack has grown up so much that the rotor cannot withstand the applied forces.

1.3 CONDITION MONITORING METHODS

Condition monitoring is the process which predicts the present and future conditions of the machinery when in operation. It gathers the information about internal effects of the operating machine. Main methods of condition monitoring are (Randall, 2011):

1.3.1 Vibration Analysis

Vibrations are always produced by machines even though they are in good conditions, this is due to periodic events in the machine's operation, such as rotating shafts, meshing gear teeth, rotating electric fields, and so on. The frequency of occurrence of such events often gives a direct indication of the source and thus many powerful diagnostic techniques are based on frequency analysis. Some vibrations are due to events that are not completely phase locked to shaft rotations, such as combustion in internal combustion (IC) engines, but where a fixed number of combustion events occur in each engine cycle, even though not completely repeatable. Other vibrations are linked to fluid flow, as in pumps and gas turbines, and these also have particular, quite often unique, characteristics. Another type of vibration which carries diagnostic information is tensional vibration, that is, angular velocity fluctuations of the shafts and components such as gears and rotor discs.

1.3.2 Oil Analysis

This can be divided in to three categories:

(a) *Chip Detectors*

Filters and magnetic plugs are designed to retain chips and other debris in circulating lubricant systems and these are analyzed for quantity, type, shape, size, and so on. Alternatively, suspended particles can be detected in flow past a window.

(b) *Spectrographic Oil Analysis Procedures (SOAP)*

In this procedure, the lubricant is sampled at regular intervals and subjected to spectrographic chemical analysis. Detection of trace elements can tell of wear of special materials such as alloying elements in special steels, white metal or bronze bearings, and so on. Another case applies to oil from engine crankcases, where the presence of water leaks can be indicated by a growth in NaCl or other chemicals coming from the cooling water. Oil analysis also includes analysis of wear debris, contaminants and additives, and measurement of viscosity and degradation. Simpler devices measure total iron content.

(c) *Ferrography*

This represents the microscopic investigation and analysis of debris retained magnetically (hence the name) but which can contain non-magnetic particles caught up with the magnetic ones. Quantity, shape and size of the wear particles are all important factors in pointing to the type and location of failure.

Proper use of oil analysis requires that oil sampling, changing and procedures are all well-defined and documented (Randall, 2011). It is much more difficult to apply lubricant analysis to grease lubricated machines, but grease sampling kits are now available to make the process more reliable.

1.3.3 Performance Analysis

With certain types of machines, performance analysis (e.g. stage efficiency) is an effective way of determining whether a machine is functioning correctly. One example is given by reciprocating compressors, where changes in suction pressure can point to filter blockage, valve leakage could cause reductions in volumetric efficiency, and so on. Another is in gas turbine engines, where there are many permanently mounted transducers for process parameters such as temperatures, pressures and flow rates, and it is possible to calculate

various efficiencies and compare them with the normal condition, so-called ‘flow path analyses.

With modern IC engine control systems, for example for diesel locos, electronic injection control means that the fuel supply to a particular cylinder can be cut off and the resulting drop-in power compared with the theoretical.

1.3.4 Thermography

Sensitive instruments are now available for remotely measuring even small temperature changes, in particular in comparison with a standard condition. At this time, thermograph is used principally in quasi-static situations, such as with electrical switchboards, to detect local hot spots and to detect faulty refractory linings in containers for hot fluids such as molten metal.

So-called ‘hot box detectors’ have been used to detect faulty bearings in rail vehicles, by measuring the temperature of bearings on trains passing the wayside monitoring point. These are not very efficient, as they must not be separated by more than 50 km or so, because substantial rise in temperature of a bearing only occurs in the last stages of life, essentially when ‘rolling’ elements are sliding. Monitoring based on vibration and/or acoustic measurements appears to give much more advance warning of impending failure.

1.4 TYPES AND BENEFITS OF VIBRATION ANALYSIS

1.4.1 Benefits as Compared to other Methods

Vibration analysis is the most prevalent method for machine condition monitoring because it has a number of advantages compared with the other methods.

(1) It reacts immediately to change and can therefore be used for permanent as well as intermittent monitoring. With oil analysis for example, several days often elapse between the collection of samples and their analysis, although some online systems do exist. Also in comparison with oil analysis, vibration analysis is more likely to point to the actual faulty component, as many bearings, for example, will contain metals with the same chemical composition, whereas only the faulty one will exhibit increased vibration.

(2) Most importantly, many powerful signal processing techniques can be applied to vibration signals to extract even very weak fault indications from noise and other masking signals.

1.4.2 Types of Vibration Analysis

(a) *Permanent Vibration Analysis*

Critical machines often have permanently mounted vibration transducers and are continuously monitored so that they can be shut down very rapidly in the case of sudden changes which might be a precursor to catastrophic failure. Even though automatic shutdown will almost certainly disrupt production, the consequential damage that could occur from catastrophic failure would usually result in much longer shutdowns and more costly damage to the machines themselves. Critical machines are often 'spared', so that the reserve machines can be started up immediately to continue production with a minimum of disruption (Randall, 2011). Most critical high-speed turbo machines, for example in power generation plants and petrochemical plants, have built-in proximity probes which continuously monitor relative shaft vibration, and the associated monitoring systems often have automatic shutdown capability. Where the machines have gears and rolling element bearings, or to detect blade faults, the permanently mounted transducers should also include accelerometers.

Advantages

(1) It reacts very quickly to sudden change and gives the best potential for protecting critical and expensive equipment.
(2) It is the best form of protection for sudden faults that cannot be predicted. An example is the sudden unbalance that can occur on fans handling dirty gas, where there is generally build-up of deposits on the blades over time. This is normally uniformly distributed, but can result in sudden massive unbalance when sections of the deposits are dislodged.

Disadvantages

(1) The cost of having permanently mounted transducers is very high and so they can only be applied to the most critical machines in a plant.
(2) Where the transducers are proximity probes, they virtually have to be built into the machine at the design stage, as modification of existing machines would often be prohibitive.

(3) Since the reaction has to be very quick, permanent monitoring is normally based on relatively simple parameters, such as overall RMS or peak vibration level and the phase of low harmonics of shaft speed relative to a 'key phasor', a once-per-rev pulse at a known rotation angle of the shaft. In general such simple parameters do not give much advance warning of impending failure.

(b) *Intermittent Vibration Analysis*

Instead of using permanent monitoring of the working machines intermittent monitoring can be done at the short intervals of time, typically once per day instead of once per week or once per month. A very large number of machines can then be monitored intermittently with a single transducer.

Advantages

(1) Much lower cost of monitoring equipment.
(2) The potential (through detailed analysis) to get much more advance warning of impending failure and thus plan maintenance work and production to maximize availability of equipment.
(3) It is thus applied primarily where the cost of lost production from failure of the machine completely outweighs the cost of the machine itself.

Disadvantages

(1) Sudden rapid breakdown may be missed and in fact where failure is completely unpredictable this technique should not be used.
(2) The lead time to failure may not be as long as possible if the monitoring intervals are too long for economic reasons. This is in fact an economic question, balancing the benefits of increased lead time against the extra cost of monitoring more frequently.

1.5 VIBRATION MEASURING INSTRUMENTS

Transducers exist for measuring all three of the parameters in which lateral vibration can be expressed, namely displacement, velocity and acceleration.

1.5.1 Velocity Transducer

There exist some transducers which give a signal proportional to absolute velocity. They are effectively a loudspeaker coil in reverse and typically have a seismically suspended coil in the magnetic field of a permanent magnet attached to the housing of the transducer (as in Figure1.3) or the inverse, where the coil is rigidly attached to the housing and the magnet seismically suspended. A body is said to be seismically suspended when it is attached to another by a spring such that when the second body is vibrated, the first will move with it at low frequencies, but when the excitation frequency exceeds the natural frequency of the suspended mass on its spring, it will remain fixed in space, and the second body will move around it. When the housing of the transducer (or pickup) is attached to a vibrating object, the relative motion between it and the seismically mounted component (for frequencies above the suspension resonance) is equal to the absolute motion of the object in space (Randall, 2011). To avoid problems with excessive response to excitation in the vicinity of the resonance frequency, the damping of the suspension is usually quite high, typically of the order of 70% of critical damping, and this also means that the amplitude response of the transducer is reasonably uniform almost down to the resonance frequency.

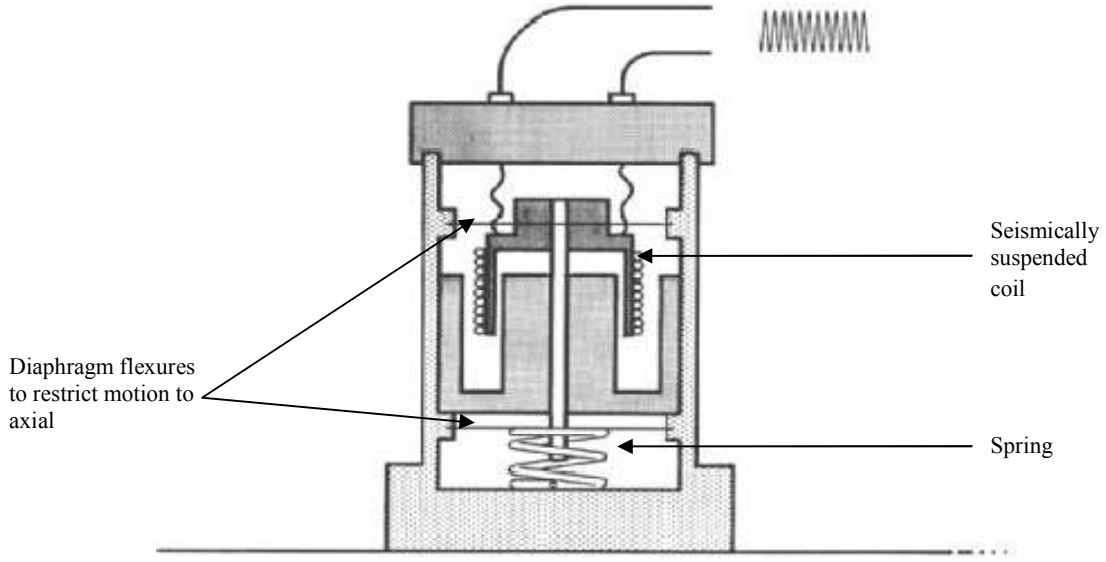

Figure 1.3 Schematic diagram of a Velocity Transducer (pickup) (Randall, 2011)

1.5.2 Accelerometer

Accelerometers are transducers which produce a signal proportional to acceleration. By far the most common types for use in machine condition monitoring are piezoelectric accelerometers, which make use of the piezoelectric properties of certain crystals and ceramics. Such piezoelectric elements generate an electric charge proportional to strain. In a typical design as shown in Figure 1.4(a), a so-called 'compression' type, the piezoelectric elements are sandwiched between a mass and the base, the whole assembly being clamped in compression via a spring.

When the base of the accelerometer is connected to a vibrating object, the mass is forced to follow the motion of the base by the piezoelectric elements, which act as a very stiff spring. The varying inertial force of the mass causes the piezoelectric elements to deform slightly, giving a strain proportional to the variation in acceleration. They then produce an electric charge proportional to this acceleration, and so their sensitivity is quoted in picocoulombs per meter per second square, pC/(m s^2).

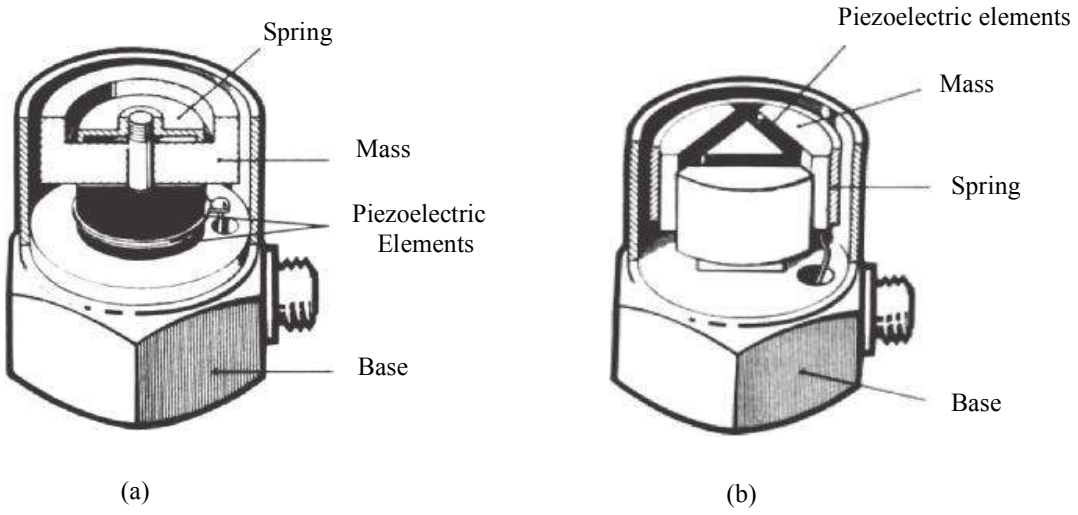

Figure 1.4 Typical accelerometer designs: (a) compression type, (b) shear type (Randall, 2011)

Figure 1.4(b) shows an alternative design where the piezoelectric elements deform in shear (they must be polarized so as to produce a charge proportional to shear rather than compressive strain).The spring in this case is a cylindrical clamping spring, once again to maintain positive compressive forces between the masses, the elements and the centre post.

Other shear designs exist, where the piezoelectric elements are clamped in one direction against a rectangular centre post, but this has the disadvantage of different transverse resonance frequencies in different directions. Another isotropic design uses cylindrical elements and masses, but these must then be cemented together, giving lower structural integrity and temperature limitations.

1.5.3 Dual Vibration Probes

Shaft vibration is normally measured by proximity probes, but this gives the motion relative to the housing. To obtain the absolute motion of the shaft, it is necessary to add this relative motion to the absolute motion of the housing, and so-called 'dual probes' are designed to do this. They contain both a proximity probe and a seismic probe to measure the absolute motion of the housing. The seismic probe can be either a velocity transducer (with signal integrated to absolute displacement) or an accelerometer (with signal double integrated to absolute displacement). The overall frequency and dynamic ranges of the combination would normally be limited by the proximity probe, so it could be said that the accelerometer gives no particular advantage over the velocity probe, but on the other hand the accelerometer signal could be separately analyzed in its own right, in which case it could give some advantage.

The ratio of relative to absolute vibration varies widely from machine to machine, and so where it is important to know how the shafts of adjacent machines are vibrating (because they have to be connected by a coupling, for example) then this has to be on the basis of overall absolute motion, as produced by a dual probe.

1.5.4 Laser Vibrometers

In recent years there has been a rapid development of vibration transducers based on the laser Doppler principle. In this technique, a coherent laser beam is reflected from a vibrating surface and is frequency shifted according to the absolute velocity of the surface (in the direction of the beam) by the Doppler Effect. The frequency shift is measured by an interferometer and converted to velocity. Note that because the frequency shift occurs at the reflection, the results virtually independent of the motion of the transmitter/receiver; in other words, it measures absolute rather than relative motion.

Laser micrometers have the big advantage that they do not load the measurement object, and the measurement point can be changed easily and rapidly by deflecting the light beam. This is

useful for making repeatable measurements over a grid in the minimum time possible. For this reason, they are now used extensively for modal analysis measurements and perhaps to a lesser extent for operational deflection shape (ODS) measurements (Randall, 2011).

1.5.5 Proximity Probes

Proximity probes measure the relative motion between a shaft and casing or bearing housing (as illustrated in Figure 1.5). It is important to realize that this gives very different information from the absolute motion of the bearing housing, as measured by a so-called 'seismic transducer's exemplified by an accelerometer. These two parameters are probably as different as the temperature and pressure of steam, even though sometimes related.

The relative motion, in particular for fluid film bearings, is most closely related to oil film thickness, and thus to oil film pressure distribution. It is thus also very important in rotor dynamics calculations, as these are greatly influenced by the bearing properties, which gives further references on fluid film bearings and rotor dynamics. However, a fluid film bearing is a very nonlinear spring, and therefore the amplitude of relative vibration does not give a direct measure of the forces between the shaft and its bearing. An increase in static load, for example, causes the oil film to become thinner, and the bearing stiffer, with reduced vibration amplitude, even though the higher load might be more likely to cause failure. (Randall, 2011)

The absolute motion of the bearing housing, on the other hand, responds directly to the force applied by the shaft on the bearing and since the machine structure tends to have linear elastic properties, the vibration amplitude will be directly proportional to the force variation, independent of the static load.

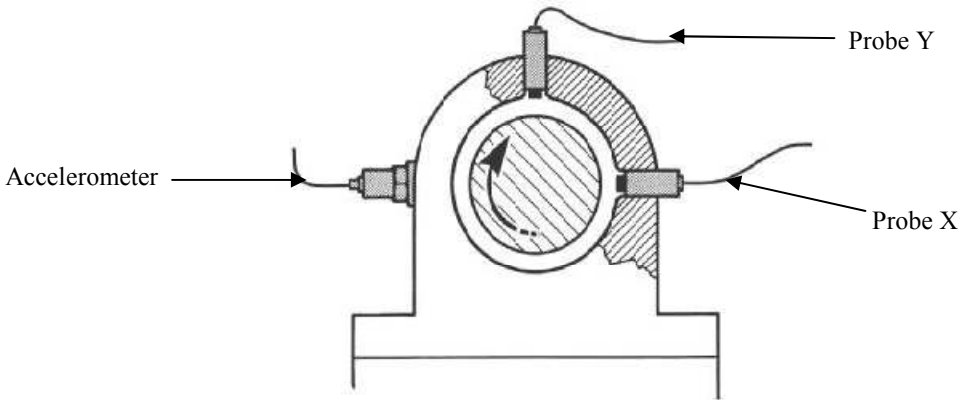

Figure 1.5 Proximity Probes installed in bearing cap (Randall, 2011)

1.6 ORGANIZATION OF THESIS

This thesis is lined in five chapters:

Chapter 1 contains the introduction part. In which there is description of various types of defects in the shafts. Firstly detailed review of cracks is given and then about other defects. Then explanation of condition monitoring and different methods of condition monitoring is imparted. Thirdly, explained about the vibration measurement equipments.

Chapter 2 concerns with the survey of published literature, in which main focus is on the vibration responses of the rotors having cracks and other defects like bend in the shaft, misalignment in the shafts and also on the response surface methodology (RSM).

Chapter 3 gives the problem formulation

Chapter 4 pertains to experimentation done on the rotor bearing system by using defective shafts. In this first of all explanation about the experimental setup is given and then explained about the dynamic analysis of rotor bearing system, after that about analysis by using Response Surface Methodology (RSM) is given in detail.

Chapter 5 provides a comprehensive discussion and conclusions arising out of the present work. The scope of the future work is also presented in this chapter.

Chapter 2
LITRETURE REVIEW

Damage detection in rotor systems is an important concern to engineering communities. Since unpredictable occurrence of damage may results in catastrophic failure, early detection of cracks become a challenging problem for researchers from several decades. It is very difficult but also highly desirable to pursue effective engineering solutions to detect and locate the damage situation in rotating systems at the earliest possible stage. Significant amount of research has been conducted in the area of defect detection in rotor systems using theoretical modelling and experimental method.

Mayes and Davies (1976) studied the vibrational behaviour of a rotating system containing a transverse crack. They further analyzed the response of a multi-rotor-bearing system containing a transverse crack in a rotor (Mayes and Davies, 1984; Davies and Mayes, 1984).

Chan and Lai (1995) studied about the digital simulation of a rotating shaft with a transverse crack. This article presented the structure of a digital computer program that was developed for this purpose. The equations of motion of the cracked shaft were solved in order to determine the dynamic response during start-up of a turbo-generator. From the simulation results, it was found that great similarities exist between the vibration behaviour of a cracked rotor and an asymmetric rotor. Both showed resonance around the half subcritical speed and the critical speed. However, resonance around one-third of the critical speed was found only in vibration of a cracked rotor. This ultra harmonic resonance was characteristic of the cracked rotor and did not occur with an asymmetric rotor.

Wu and Huang (1998) examined about the vibration of a shaft-disk rotor containing a transverse crack and supported by speed-dependent bearings**.** In this an energy approach was employed that included the crack-released energy for the vibration analysis of shaft-disk-bearing rotors containing a transverse crack. The bearings were characterized by speed-dependent stiffness and damping. The paper presented a valuable approach for the vibration, and the crack-detection analysis of rotor systems. From the derivation and numerical results following conclusions were given: (a) the response amplitude was

proportional to the crack depth and the bending moment at crack location. (b) Response measured by one probe cannot provide sufficient information for crack identification. By using the technique of intersections of equi-amplitude contours from multi probes, the crack location and depth can be identified.

Prabhakar et al. (2001). looked into the detection and monitoring of cracks in a rotor-bearing system using continuous wavelet transforms (CWT) during start-up and shut-down conditions. In this experiment a steel shaft supported on two isotropic flexible bearings at both ends and having a disc at the centre and crack near to it was analyzed. A large increase in amplitudes of vibration was observed with the cracked rotor compared to the un-cracked rotor in both the response plots. However, the characteristic subcritical response peaks at half and one fourth the critical speed could be clearly observed only in the CWT of the cracked rotor bearing system.

Darpe et al. (2003 (a)) did experimentation on simple Jeffcott rotor with two transverse surface cracks. The stiffness of such a rotor was derived based on the concepts of fracture mechanics. Also, the effect of the interaction of the two cracks on the breathing behaviour and on the unbalance response of the rotor was studied and the main results were, When the orientation of one crack relative to the other was varied, the breathing behaviour of the cracks changed leading to the changes in the stiffness variation that ultimately affects the response pattern of the cracked rotor. The effect of the orientation of the crack on the response was more strongly observed at lower speeds.

Darpe et al. (2003 (b)) further studied about the experimental investigations of the response of a cracked rotor to periodic axial excitation. In this the coupling of lateral and longitudinal vibrations due to the presence of transverse surface crack in a rotor was explored. The following results were found:

a) In non-rotating condition, the cracked shaft shown the presence of the axial excitation frequency in the spectrum of lateral vibration thereby confirming the presence of coupling of axial and bending vibrations in the case of cracked shaft.

b) When the rotors are axially excited in the rotating condition with the frequency equal to the bending natural frequency, the bending natural frequency shown prominent presence in both horizontal and vertical lateral vibration spectra.

c) The non-linearity due to the crack is clearly observed with the presence of higher harmonics of the rotational frequency in the spectrum.

Darpe et al. (2004) gave the information about transient response and breathing behaviour of a cracked Jeffcott rotor. This rotor passed through its critical speed and sub-harmonic

resonances. Three different crack models were studied, namely, a breathing crack model, a switching crack model and an open crack model. The breathing behaviour was different for accelerating and decelerating rotors. For shallow depths and higher damping, the breathing observed at speeds away from the critical speed continues even in the critical speed zone. Peak response of the cracked rotor whilst passing through the critical speed depended on unbalance orientation angle, unbalance amount, crack depth, acceleration/deceleration rate and whether the rotor was accelerated or decelerated. For open crack model the peak response during deceleration did not vary much with crack depth.

Sabnavis et al. (2004) provided the information about the various types of the cracks and also explained about the online and offline techniques to diagnose these cracks. The important information given, was about the steps of the failure of the shaft which included crack initiation, crack propagation and failure and also guided about the various newer techniques which are emerging as further insight is gained in the fields of fracture mechanics, simulation and condition monitoring.

Sekhar et al. (2005) analysed the difference between transverse and slant cracks. The difference expressed that transverse crack breaths with a frequency equal to rotation of shaft (ω) whereas slant Crack breaths with a frequency equal to torsional excitation frequency (ω_T). In transverse crack FFT shows the characteristic features of 1X, 2X, 3X components of frequency equal to the rotor speed while in slant crack FFT shows the sub- and super harmonic frequency components at an interval frequency corresponding to tensional frequency cantering on the rotor running frequency. In transverse crack the normalized mechanical impedance is highly sensitive to crack depth where in slant crack the normalized mechanical impedance is relatively less sensitive to crack.

Sinou and Lees (2005) observed the influence of transverse cracks on the rotating shaft. It addressed the two distinct issues of the changes in modal properties and the influence of crack breathing on dynamic response during operation and also investigated the evolution of the orbit of a cracked rotor near half of the first resonance frequency. In this online monitoring method was used. In order to conduct this study, the dynamic response of a rotor with a breathing crack was evaluated by using the Alternate Frequency Time domain approach. During this experiment this result was found that when the crack depth increases, then orbit amplitude also increases, as well as a decrease of the shaft speed at which the 2X harmonic component of the dynamic response is maximum. In this the use of the AFT domain method and a path-following procedure allows us to obtain rapidly and

efficiently the nonlinear dynamical behaviour of a rotating shaft with a transverse breathing crack. This method has advantages in terms of commutating time.

Mania et al. (2006) studied about the Active health monitoring in a rotating cracked shaft using active magnetic bearings as force actuators. In this the active health monitoring of rotor dynamic systems in the presence of breathing shaft cracks was considered. The shaft was assumed to be supported by conventional bearings and an active magnetic bearing (AMB) was used in a mid-shaft or outboard location as an actuator to apply specified, time-dependent forcing on the system. Through the method of multiple scales a combination resonance was identified between the critical frequency of the shaft, the operating speed of the shaft, and the frequency of the AMB excitation. Therefore, because the excitation frequency can be chosen arbitrarily, this resonance condition can be satisfied for any combination of critical shaft frequency and operating speed.

Pennacchi et al. (2006) gave the information about a model-based identification method of transverse cracks in rotating shafts which is suitable for industrial machines. In this three different types of cracks were considered: the first was a slot, which was not actually a crack since it had not the typical breathing behaviour, the second a small crack(14% of the diameter of the shaft) and the third a deep crack (47% of the diameter of the shaft).The excellent accuracy obtained in identifying position and depth of different cracks proved the effectiveness and reliability of the proposed method.

Darpe (2007 (a)) studied a novel way to detect transverse surface crack in a rotating shaft. The method which was used showed both the typical nonlinear breathing phenomenon of the crack and the coupling of bending–torsional vibrations due to the presence of crack for its diagnosis. During experimentation transient torsional excitation was applied for a very short duration at specific angle of the rotor and its effect in the lateral vibrations was investigated. Variation of peak absolute value of wavelet coefficient with that angle at which torsional excitation was applied was investigated. The correlation of this variation with the breathing pattern of the crack was studied. The sensitivity of the proposed methodology to the depth of crack was analyzed and this analysis shown that the peak absolute value of wavelet coefficient was highly sensitive to the depth of crack and even a very shallow crack (5% of rotor diameter) can be detected.

Darpe (2007 (b)) further demonstrated regarding the Coupled vibrations of a rotor with slant crack. There was a comparison between rotor with slant and transverse crack with regard to the stiffness coefficients and coupled vibration response characteristics. The comparison of stiffness coefficients derived in this paper with those of transverse crack

revealed that the slant crack exhibited a very strong cross-coupling of torsional and other modes of vibration (bending and longitudinal). This was revealed in larger torsional vibration to lateral unbalance excitation in the case of slant crack. The new stiffness matrix derived here showed a fully populated stiffness matrix for slant crack as additional SIFs are introduced due to orientation of the crack to shaft axis.

Sinou and Lees (2007) analyzed about the non-linear study of a cracked rotor and gave the information about influence of crack opening and closing on dynamic response during operation. The evolution of the orbit of the cracked rotor near half and one-third of the first critical speed was investigated. The study gave the results that the introduction of a deep breathing crack increased the $2X$ and $3X$ harmonic component of the system response. The behaviour of the $2X$ harmonic component of the system response increased in magnitude when the crack depth increased. Moreover, the primary response characteristic resulting from the changes in the non-linear dynamical behaviour of the rotor system through half resonance speeds appeared to be the characteristic signature for detecting the presence of a crack rotor.

Lees (2007) gave the information about the misalignment between the two rotors which also demonstrated the vibrational behaviour. This paper gave the following results:

a) Using a purely linear model, the equations of motion of a machine with a coupling alignment fault were derived.

b) Solutions for some simple cases were given both analytically and numerically.

c) It was shown that the linear model generates responses at harmonics of shaft speed.

d) The harmonics were caused by an interaction of torsional and flexural effects.

e) The combination of these mechanisms with the nonlinearities of a real system can explain the confusion in the literature.

Khalid et al. (2007) provided the information about the Bending fatigue behaviour of hybrid aluminum/composite drive shafts. In this experiment the hybrid shafts were made by using filament winding technique. Glass fibre with a matrix of epoxy resin and hardener were used to construct the external composite layers of the shaft and also different stacking sequences were used to laminate the shafts and following results were found:

(a) Increasing the number of composite layers would increase the fatigue strength for a hybrid aluminum/ composite drive shaft.

(b) Aluminum shafts with laminates of a stacking sequence [+/45/_45]3s have the highest fatigue strength, up to 40% when compared to others.

Sinou (2008) studied the detection of cracks in rotor based on the 2*X* and 3*X* super-harmonic frequency components and the crack–unbalance interactions. Due to crack–unbalance interaction the evolutions of the super-harmonic frequency components and the associated resonance peaks were very complex. It was demonstrated that for a given crack depth, the unbalance did not only affect the vibration amplitudes of the 1*X* amplitudes, but also the 1/2 and 1/3 sub-critical resonant peaks. When the unbalance magnitude was increased, then 1/n sub-critical resonant peaks increased obviously due to the non-linear behaviour of the breathing crack and the interaction between the crack, gravity and unbalance of the rotor.

Bachschmid et al. (2008) examined about the effect of helicoidal cracks on the behaviour of rotating shafts. A 3D model for helicoidal crack was used for calculating breathing behaviour and deflections of a cracked specimen loaded with bending and torsion loads. Then these were compared to transverse crack model results, showing generally only small differences between the two cases, in different loading conditions. It was shown that torsion loads emphasize these differences and also Torsion loads increase deflections, when (positive) torsion opens the crack and lowers consequently the stiffness. When torsion was absent then the torsional deflection was rather strongly excited by the bending through coupling mechanism, much more with respect to the flat transverse crack.

Papadopoulos (2008) studied the strain energy release approach for modelling cracks in rotors. In this the SERR theory was applied to a rotating crack and gave good results. A specific behaviour was expected when a fluid was inserted between the ‘‘breathing’’ lips of the crack. The effect of the cracks on thermal phenomena and on the increase of the hysteretic was investigated. The hysteretic damping of a cracked vibrating shaft changed and this change could be connected to the position and depth of the crack. The hysteretic damping greatly affected the stresses of a vibrating structure or of a rotating shaft.

Babu and Sekhar (2008) told about the Detection of two cracks in a rotor-bearing system using amplitude deviation curve (ADC). This is also called slope deviation curve (SDC) which was a modification of the operational deflection shape (ODS). The effectiveness of the SDC over ODS for small cracks detection was demonstrated in the present paper. Therefore, online detection of crack parameters by the present method can prove to be a good tool in detecting even small cracks around 10% (depth of crack to shaft diameter).

Patel and Darpe (2008) examined about the vibration response of a cracked rotor in presence of rotor–stator rub. In this numerical simulations and experimentations were carried out and vibration signals were analysed using full spectrum analysis. It was

observed that the relative phase information between the vibration signals in two directions was important to relate the nature of vibration excitations with the rotor faults. The present study showed that full spectrum utilizes this directivity information of the rotor orbit and effectively revealed the whirl nature of the excitation frequencies. Excitations due to unbalance and crack were strongly forward whirling in nature. Vibration motion at 2*X* harmonic was strongly forward in cracked rotor, in comparison with vibrations at 1*X*, 3*X*, and 5*X* harmonics.

Patel and Darpe (2009 (a)) provided the information about the Study of coast-up vibration response for rub detection. In these two different rubbing conditions, i.e. heavy rub and light rub were observed and it was concluded that rotor–stator interactions were highly nonlinear and exhibit a complex vibration response. Rotor– stator contact increased the effective stiffness of the system and hence the shift in resonance speed was observed. More severe the rub condition more was the shift in resonance speed. The Hilbert–Huang transform (HHT) was found effective in revealing the nonlinear nature of the non-stationary rub vibration signals. The HHT of rub signal showed vibration response rich in sub-synchronous and super synchronous frequencies and their content was precisely located in time.

Patel and Darpe (2009 (b)) further analyzed the experimental investigations on vibration response of misaligned rotors. In this influence of misalignment and its type on the forcing characteristics of flexible coupling was investigated followed by experimental investigation of the vibration response of misaligned coupled rotors supported on rolling element bearings. Firstly the rotor was having no misalignment and in second case having misalignment. Then after experimentation various forces were measured and it was concluded that the presence and type of misalignment (parallel and angular misalignment) had significant influence on harmonic content of the misalignment excitation forces.

Patel and Darpe (2009 (c)) again demonstrated the experimental approach for determination of magnitude and harmonic nature of the misalignment excitation. This gave the information about the simulation of FE model using nodal force vector. In this work, the influence of types of misalignment on the rotor vibration behaviour was investigated in detail. In addition to the vibration waveforms, orbit plots and conventional one-sided Fourier transforms, two-sided spectrum (full spectrum) was effectively used to identify unique vibration features related to the misalignment fault.

Patel and Darpe (2009 (d)) gave the information about the Coupled bending-torsional vibration analysis of rotor with rub and crack. In this paper, modelling and vibration

signature analysis of rotor with rotor–stator rub, transverse fatigue crack and unbalance were analyzed. The rotor–stator interaction effects on the response of a rotor were investigated in the presence/absence of a transverse crack. Form this study it was observed that the torsional response of the cracked rotor was strong in 1*X* and 2*X* frequencies. The higher order frequencies were relatively weak and torsional response of cracked rotor in presence of rub exhibited strongvibrationsat1*X* as well as at torsional natural frequency.

Dong et al. (2009) studied, a method based on high-precision modal parameter identification method and wavelet finite element (WFE) model was presented to determine the depth and location of a transverse surface crack in a rotor system and additionally, a novel method based on empirical mode decomposition (EMD) and Laplace wavelet was proposed to acquire modal parameters with high precision, which was implemented to improve the precision of crack identification and it was concluded that results of simulative signals and experimental signals indicated that the proposed method can identify frequency and damping ratio accurately. The relative error in identifying the location of a crack was less than 3% and the relative error of crack size was less than 4%.

Chasalevris and Papadopoulos (2009) investigated the problem of coupled bending vibrations in a cracked rotor mounted in resilient bearings. The method in this study offered a continuous model for a cracked rotor-bearing system, including three parameters of coupling: (a) the coupled equations of motion, (b) the coupling due to the breathing crack and (c) the coupling due to cross-coupled bearing coefficients for stiffness and damping and following results were obtained:

a) The coupling affected the response in the time and frequency domains and amplified the higher harmonics that the crack introduced as components in the vibration.

b) The resilient bearing analysis, including cross-coupling stiffness and damping coefficients, provided evidence that the coupling due to a crack was negligible in respect to the coupling that the bearings introduced.

c) The higher harmonics that were introduced in the vibration spectrum due to the stiffness change caused by the breathing of the crack clearly indicated the existence of a crack since the amplification of 2*X* rev harmonic amplitude was increased from the crack cross-coupling compliances.

Elforjani and Mba (2009) studied the detection of natural crack initiation and growth in slow speed shafts with the Acoustic Emission technology. A special purpose built test rig was employed for generating natural degradation on a shaft. Various tests were performed and these tests demonstrated the applicability of AE in detecting crack initiation and

propagation on slow speed shafts while in operation. It was concluded that there was a clear correlation between increasing AE energy levels and the natural propagation and formation of shaft defects. The study had also demonstrated that AE parameters such as counts; amplitude and ASL were reliable, robust and sensitive to the detection of natural cracks and surface damages in slow speed shaft. This work was the first known attempt at correlating AE activity and natural defect generation in slow speed rotating shafts and it was also the first known attempt at monitoring the mechanical integrity of rotating shafts.

Kankar et al. (2009) concluded the Fault diagnosis of a rotor bearing system using response surface method. This method was utilized to analyze the effects of design and operating parameters on the vibration signature of a rotor-bearing system. Form this study following results were found: a) Nonlinear dynamic responses were found to be associated with large internal radial clearance and distributed defects. b) The system indicated periodic nature, when ball waviness was at its maximum level. c) It was shown that the system exhibited dynamic behaviours which were extremely sensitive to small variations of the system parameters, such as internal radial clearance and ball waviness.

Han (2009) concluded the Vibration analysis of periodically time-varying rotor system with transverse crack. In this the vibration analysis associated with modal characteristics, whirling, instability, directional frequency response functions (dFRFs) and directional spectrum (dS) was carried out, Which was strongly indicating the effect of the crack growth so that the presence or the propagation of the crack could be effectively identified.

Lin and Chu (2010) studied the dynamic behaviour of a rotor system with a slant crack on the shaft. The slant crack had an angle of 45°. This also told about the comparison of slant crack, open transverse crack . Following results were found:

a) The slant crack caused coupling stiffnesses of bending–torsion, bending–tension and torsion–tension on the shaft; and the transverse crack had coupling stiffnesses of bending–tension on the shaft.

b) For the transverse-cracked shaft, since there were bending–tension coupling of the stiffnesses and bending–torsion coupling caused by the eccentricity, tension–torsion coupling will exist also due to the interaction of couplings. Even then, the slant-cracked shaft manifests much stronger bending–torsion and tension–torsion coupling vibrations than the transverse-cracked one since besides eccentricity caused.

Bachschmid et al. (2010) examined the dynamic behaviour of heavy, horizontal axis, turbo generator units affected by transverse cracks in the frequency domain by means of a quasi linear approach, using a simplified breathing crack model applied to a traditional finite

element model of the shaft-line. This allowed to perform a series of analyses with affordable computational efforts and gave following results:

a) Crack forces depend on depth and are proportional to the static bending moment divided by the third power of the shaft diameter.

b)The excitation of maximum vibrations at a given rotating speed per unit crack force occurs when the corresponding mode shape presents high curvature in correspondence to the crack position.

c) The maximum response occurs obviously in resonant conditions with 1*X*, 2*X* and 3*X* critical speeds.

Freitas et al. (2010) investigated about the effect of steady torsion on fatigue crack initiation and propagation under rotating bending. This effect was studied for both small and long crack growth. For this experiment replica's method was used to monitor crack initiation and small crack growth of the Ck45 steel specimens under multiaxial fatigue loading conditions. An effective-strain intensity factor range based on the corrected strain range parameter through the use of non-proportional loading effect and additional cyclic hardening coefficient was proposed. This parameter was used to correlate the small crack growth rate data. The correlation achieved was reasonable and consistent with long crack data and could be considered a useful tool for calculation of fatigue life.

Cheng et al. (2011) studied the influence of crack breathing and imbalance orientation angle on the characteristics of the critical speed of a cracked rotor. The dynamic response of a cracked rotor near its critical speed was computed with a numerical method to investigate the influence of nonlinear breathing of the crack and that of the imbalance orientation angle β on the stability, critical speed and peak response of the rotor. The results pointed that nonlinear breathing can improve the stability of a rotor in contrast to a rotor with an open crack ,and ,with a reversed imbalance ($70<\beta<270$), that it can reduce the vibration response in contrast to an un-cracked rotor. The basic characteristics of a cracked rotor near its critical speed were similar to those of an un-cracked rotor.

Rubio et al. (2011) analyzed the Static behaviour of a shaft with an elliptical crack. In this experiment flexibility expressions for cracked shafts having elliptical cracks were obtained, based on the polynomial fitting of the stress intensity factors, taking into account the size and shape of the elliptical cracks showing results according with reality. The static displacements in bending of the shaft for different support conditions had been calculated. The comparisons between these results and those obtained by FEM analysis and by

experimental tests expressed that the closed-form expressions for the flexibility gave a very good approximation to the behaviour of the cracked shaft.

In previous published articles, research has been done in the area of crack detection in systems using theoretical modelling method as well as experimental methods. These methods were used to examine about the changes in the rotor dynamic behaviour due to defects in shafts. Few other methods which had been used to detect defects in the rotor bearing system were Continuous Wavelet Transform (CWT) (Darpe, 2007), Hilbert–Huang Transform (HHT) (Patel and Darpe, 2009), Amplitude Deviation Curve (ADC) and Empirical Mode Decomposition (EMD). In previous papers interaction between the defects and its effect on dynamic behaviour was not much studied.

In present analysis, response surface methodology has been used to analyze the interaction between defects and also to predict amplitude of vibration in presence of defects simultaneously which is not done in the previous studies.

Chapter 3
PROBLEM FORMULATION

As demand on running accuracy and high speed machines is increased, detection of defect in rotor systems become important for engineers. Lot of research is being directed towards detection and prognosis of various types of defects in the shafts/rotors.

In previous studies, significant amount of research has been conducted in the area of crack detection in systems using theoretical modelling method as well as experimental method. These approaches analyze changes in the rotor dynamic behaviour due to defects in shafts. Exciting frequency obtained is used to detect cracks in the rotor systems. Some other methods which have been used to detect defects in the rotor bearing system are Continuous Wavelet Transform (CWT) (Darpe, 2007), Hilbert–Huang Transform (HHT) (Patel and Darpe, 2009), Amplitude Deviation Curve (ADC) and Empirical Mode Decomposition (EMD). In most of these studies work has been focused mainly detection of defects in shafts and its effect on dynamic behaviour of rotor systems. Interaction between the defects and its effect on dynamic behaviour is also not much studied.

This work mainly seeks to analyze the vibration responses of a horizontal rotor supported on ball bearings and to develop a fault diagnosis system for rotor bearing system. The sources of vibration in the rotor are the presence of different types of defects. These defects are cracks, bend shaft and misalignment. These defects are considered with different severity level. Since it is not necessary that at a time only one defect exist in the system, it is necessary to consider the changes in dynamic behaviour due to presence of different types of defects simultaneously in the rotor system. In present analysis, response surface methodology is being used to analyze the interaction between defects. RSM can be used effectively to predict amplitude of vibration in presence of defects simultaneously which is not done in the previous studies.

Chapter 4
EXPERIMENTATION

Study of dynamic behaviour of shafts of rotating machines under the influence of various defects (like bent shaft, misaligned shafts, unbalanced shafts and shafts having cracks) has been a focus of attention for many researchers. The presence of a defect may lead to a dangerous and catastrophic effect on the rotating machinery. Therefore, the timely detection of a rotor defect would potentially avoid severe damage and expensive repairs due to the failure of rotating machinery. It also helps to avoid any human causality due to catastrophic failure.

The several vibration and acoustic measurement methods have been used for the detection of defects in rotor bearing system. The vibration signals contain information of defective parts. A variety of vibration based techniques have been developed to monitor the condition of system. Vibration signals may be analyzed using time domain analysis, frequency domain analysis and time-frequency domain analysis (wavelet). In present study, frequency domain analysis is used to analyze effect of various defects of shaft on dynamic behaviour of rotor bearing system.

4.1 EXPERIMENTAL SETUP

The problem of predicting the degradation of working conditions of rotor bearing system and trending of fault propagation before they reach the alarm or failure threshold is extremely important in industries. This increases utilization of the machine production capacity and reduces the plant downtime. In the present study, experimentation is carried out on a rotor test rig. The EN8 steel rigid rotor has been taken for the study, which is supported in the healthy ball bearings (SKF 6304 ZZ). The rig is connected to a data acquisition system through proper instrumentation as shown in Figure 4.1. A piezoelectric accelerometer is used for picking up the vibration signals. Vibration responses for healthy shafts and shafts with defects are obtained. Specifications of shafts and bearing used in the experiments are given below.

Specifications of shafts

Length of the shaft = 760mm

Diameter of shaft = 21mm

Weight of the shaft = 2.5 Kg

Material of the shaft = EN8 steel

Specifications of ball bearings (SKF 6304 ZZ)

Outer diameter = 52mm

Inner Diameter = 20mm

Width of the bearing = 15mm

Number of balls = 7

4.1.1 Experimental Test Rig

The experimental rig used in this study is shown in Figure 4.1. This rig consists of a shaft supported on rolling element bearings and driven by a DC motor whose operating speed can be controlled. A flexible coupling has been used to connect shaft and motor. The design facilitates easy removal and replacement of the parts as shown in Figure 4.1.

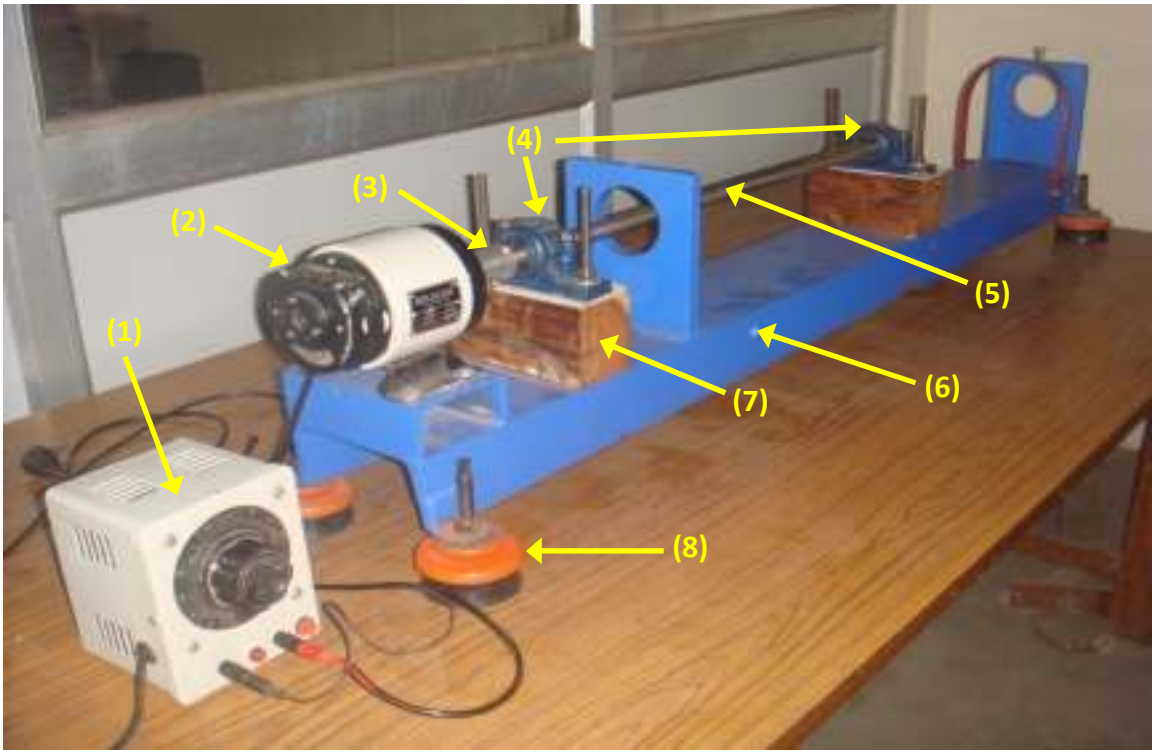

Figure 4.1 Experimental Test Rig

(1) Speed control unit, (2) DC Motor, (3) Flexible Coupling, (4) Bearing Housings, (5) Shaft

(6) Base, (7) Wooden Block, (8) Rubber Boot

4.1.2 Data Acquisition System

Data acquisition and analysis system consists of OR36 (4-16 channels) Modular Multi-Analyser/Recorder as shown in Figure 4.2. This is a dedicated system for advanced needs in vibration and acoustic analysis measurements for R&D as well as for testing. It has OROS NV Gate software in it. This instrument contains the essential functions covering the entire measurement process in a compact unit. OR36 can be used as s true data recorder with its Mobi Disk (60 GB) with or without PC and PCI data acquisition speed is (52.4 kSamples/sec). Speed of the rotor is measured with the help of Mechanical Tachometer. For picking up the vibration signals a piezoelectric accelerometer (353B34) having sensitivity of 0.00101936 is used. This accelerometer has measurement range of 0.5 to 5000 Hz. In this the optimum signals are obtained from accelerometer located at the bearing housing. Therefore, accelerometer is fitted in vertical direction on the bearing housing.

Figure 4.2 OR36 Modular Multi-Analyser/Recorder

4.2 EXCITING FREQUENCIES

Rotor bearing system is excited at different frequencies as per the condition of rotor and bearing. These exciting frequencies are:

4.2.1 Varying Compliance frequency

When the rolling element set and the cage rotates with a constant angular velocity, a parametrically excited vibration is generated and transmitted through the outer race. These vibrations are produced due to finite number of balls carrying load. The characteristic frequency of this vibration is called the varying compliance frequency (*VC*) and is given as (Kankar, 2011):

$$VC = N_b \times \omega_{cage} \tag{4.1}$$

4.2.2 Critical frequency of the shaft

The critical frequency of the shaft is the frequency at which the rotating shaft becomes dynamically unstable and starts to vibrate violently in transverse direction. This is given by (CNC Router, 2007):

$$\omega_c = \frac{N \text{ x } 4.76 \text{ x } 10^6 \text{ x } d}{L^2} = 6610 \text{ rpm} \tag{4.2}$$

N=Fixity Type

0.25 For Fix-Free ends type

1.00 For Supported-Supported type

2 for Fix-Supported end type

4 for Fixed-Fixed end type

The values of above listed frequencies are calculated and are given in the Table 4.1.

4.3 DYNAMIC ANALYSIS OF ROTOR BEARING SYSTEM

This phase deals with the non-linear dynamic response of rotor supported by ball bearings. The excitation is due to the different types of defects in the shaft or rotor, these defects are bent shaft, misaligned shaft, transverse crack and slant crack. The ball bearings used for this experimentation are healthy in nature. The present study characterizes the vibration frequencies resulting from the above listed defects.

Table 4.1 Rotational and Varying Compliance frequencies at different speeds

Speed (rpm)	Rotational Frequency (Hz)	Varying Compliance Frequency (Hz)
500	8.33	21.42
1000	16.67	42.91
1500	25	64.33
2000	33.3	86.1
2500	41.7	107.1
3000	50	128.8
3500	58.3	149.8
4000	66.7	171.5
4500	75	193.2
5000	83.3	214.2

Critical frequency of the shaft= ω_c =110.16 Hz

4.3.1 Results and Discussion

The results obtained in frequency domain using Fast Fourier Transform (FFT) for different defects are discussed below. This gives the output in the form of graph between amplitude v/s frequency. In the experiments, the rotor is supported on healthy ball bearings. In this study, different cases are considered as:

1) Response of healthy rotor/shaft.
2) Response of bent shaft.
3) Response of axial misaligned shaft (misaligned with Motor shaft).
4) Response of shaft having transverse crack (20% of diameter of shaft)
5) Response of shaft having slant crack (20% of diameter of shaft)

4.3.1.1 Response of healthy rotor/shaft

As a first step in the study of a rotor bearing system, it is essential to establish a base-line for the behavior of healthy shaft. The vibration spectrums for healthy shaft at different speeds are given in Figures 4.3 to 4.12. At 500 and 1000 rpm, the vibration responses are shown in Figure 4.3 and Figure 4.4 respectively. The peak amplitude of vibration appears on critical speed of the shaft (ω_c=110.16 Hz). Other peak appears at harmonics of varying compliance frequency ($3VC$=64.26 Hz) at 500 rpm and as an interaction of rotational

frequency and varying compliance frequency at ($6X$+$5VC$=314.57 Hz). The frequency spectrum at 1500 and 2000 rpm is shown in Figures 4.5 and 4.6. It is clear that the peak amplitude appears on the rotational frequency (X) and the multiple of varying compliance frequency. The amplitude of vibration increases as speed increase to 2000 rpm. Figure 4.7 shows the vibration response at 2500 rpm. The peak amplitude of vibration appears at rotational frequency ($2X$=83.4 Hz) and varying compliance frequency ($6VC$=642.6 Hz). The peak amplitude at 3000 rpm (Figure 4.8) is at rotational frequency ($3X$=150 Hz). Figures 4.9, 4.10 and 4.11 show frequency responses at 3500, 4000 and 4500 rpm respectively. The peak amplitude of vibration appears in vibration spectra at the rotational frequency and its multiple. The speed at 5000 rpm gives the response at rotational frequency (X=83.3 Hz) and at $4VC$=856.8 Hz. Table 4.2 show the summary of exciting frequencies for healthy shaft at various speeds.

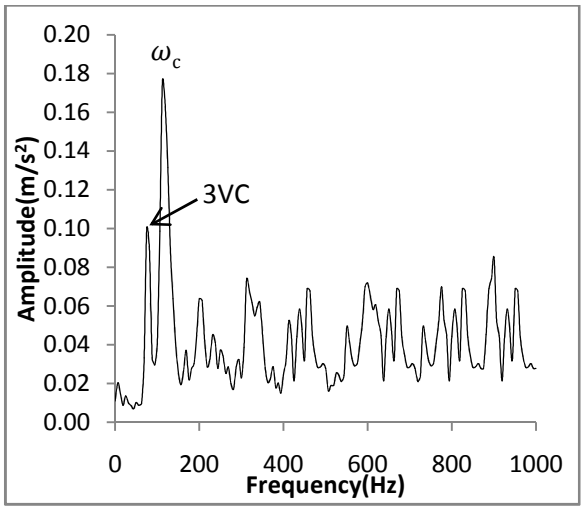

Figure 4.3 Response of healthy shaft at 500 rpm

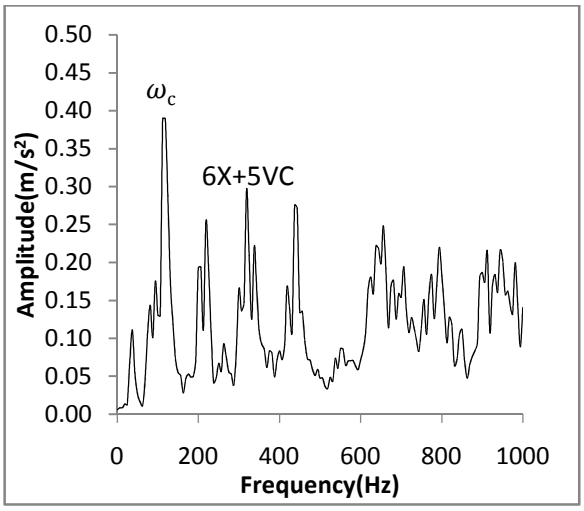

Figure 4.4 Response of healthy shaft at 1000 rpm

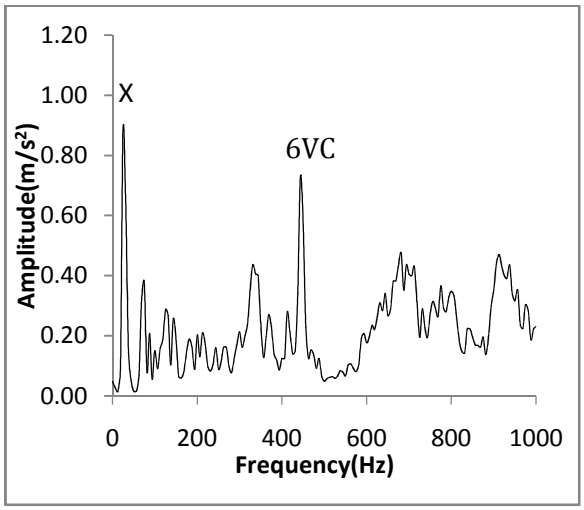

Figure 4.5 Response of healthy shaft at 1500 rpm

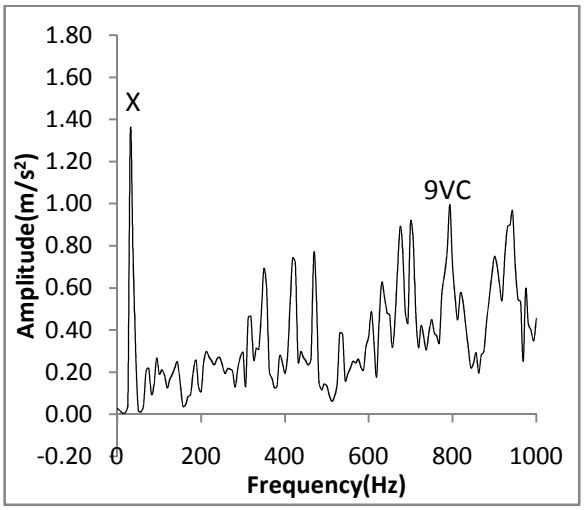

Figure 4.6 Response of healthy shaft at 2000 rpm

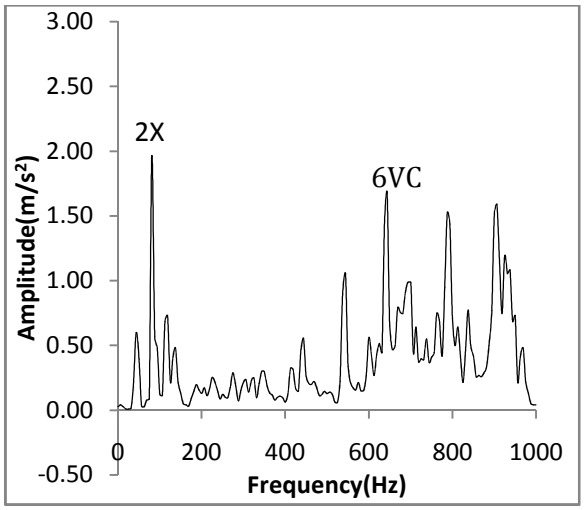

Figure 4.7 Response of healthy shaft at 2500 rpm

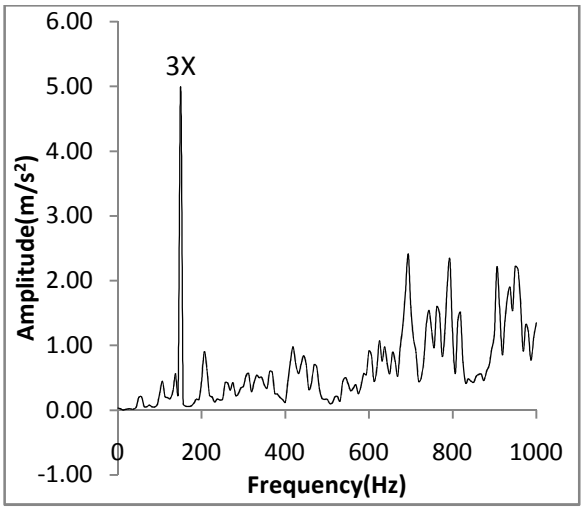

Figure 4.8 Response of healthy shaft at 3000 rpm

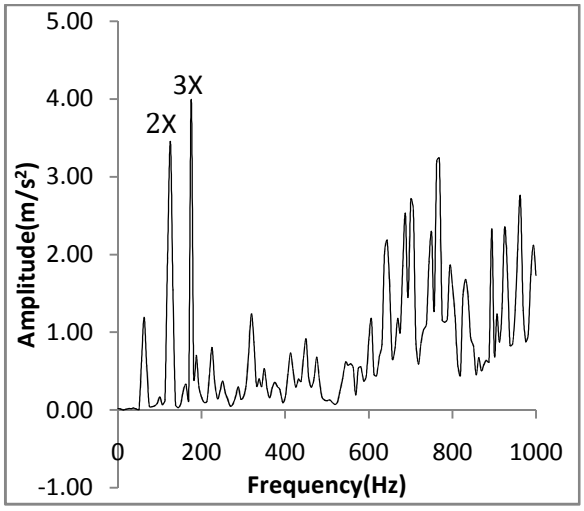

Figure 4.9 Response of healthy shaft 3500 rpm

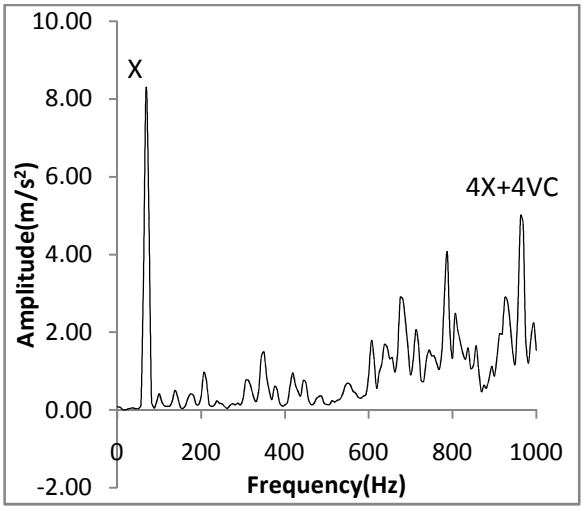

Figure 4.10 Response of healthy shaft 4000 rpm

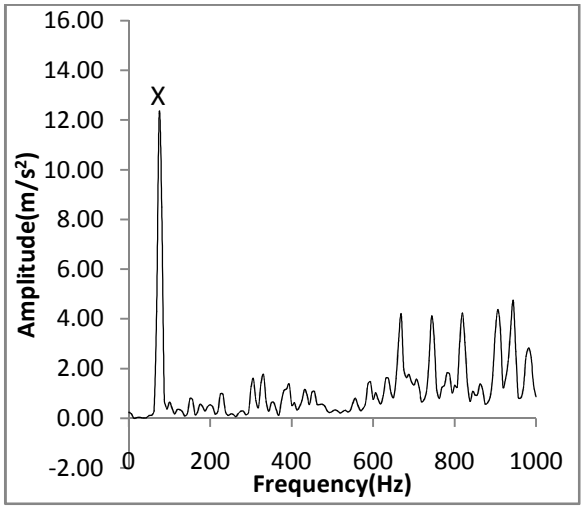

Figure 4.11 Response of healthy shaft 4500 rpm

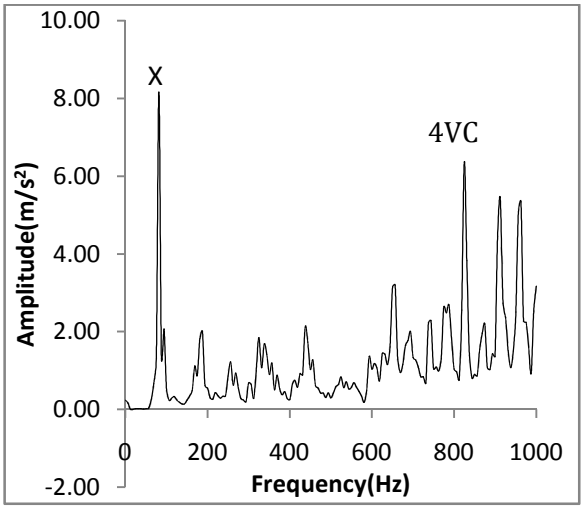

Figure 4.12 Response of healthy shaft 5000 rpm

Table 4.2 Summary of healthy shaft

Speed (rpm)	Peak Amplitude	Harmonic in shaft spectrum	Peak Amplitude Value (m/s^2)
500	ω_c	$3VC$	0.163
1000	ω_c	$6X+5VC$	0.389
1500	X	$6VC$	0.657
2000	X	$9VC$	1.34
2500	$2X$	$6VC$	1.96
3000	$3X$	-	4.99
3500	$3X$	$2X$	3.99
4000	X	$4X+4VC$	8.29
4500	X	-	12.3
5000	X	$4VC$	8.16

4.3.1.2 Response of bent shaft

In present work, vibration signatures associated with bent shafts have been studied experimentally. The vibration responses between baseline and bent under various shaft speeds from 500 to 5000 RPMs have been compared. The experiment results indicate that due to bent shaft amplitude of vibration increases considerably as compare to healthy shaft condition. This is because a bent shaft will increase bearing reaction force for both low and high speeds. The peak amplitude of vibration appears mainly at rotational frequency (X) and its multiple at ($2X$). Bend in the shaft is considered up to 3mm and response plots at speeds of 500 to 5000 rpm are shown in Figures 4.13 to 4.22 respectively. Figure 4.13 shows the frequency response at 500 rpm, which demonstrates the peak in the frequency spectrum on rotational frequency (X=8.33 Hz) and varying compliance frequency ($5VC$=118.75 Hz). The peak excitations at 1000 rpm (Figure 4.14) appear at rotational frequency and its multiple (X=16.67 Hz and $4X$=66.8 Hz). Figure 4.15 shows vibration response at 1500 rpm. The peak values of amplitude appear at rotational frequency (X=25 Hz) and varying compliance frequency ($5VC$=321.65 Hz). The response plot in the Figures 4.16, 4.17 and 4.18 show that the peak appears at twice of rotational frequency ($2X$). Other peaks appear at thrice of rotational frequency at $3X$. The amplitude of

vibration increases with speed. The peak values in the frequency spectrum at 3500 rpm comes out at twice of rotational frequency ($2X$=116.6 Hz) and varying compliance frequency ($4VC$=599.2). The nature of the response at 4000 rpm is shown in Figure 4.20. The peak amplitudes of vibration appear at rotational frequency and its multiple (X=66.7 Hz, $2X$=13.4 Hz). Response plots of in Figure 4.21 & 4.22 give the peak value at rotational frequencies (X=75 Hz and X=83.3 Hz) at 4500 and 5000 rpm respectively. The summary for the peak amplitude and harmonics in frequency spectrum for bent shaft is given in Table 4.3.

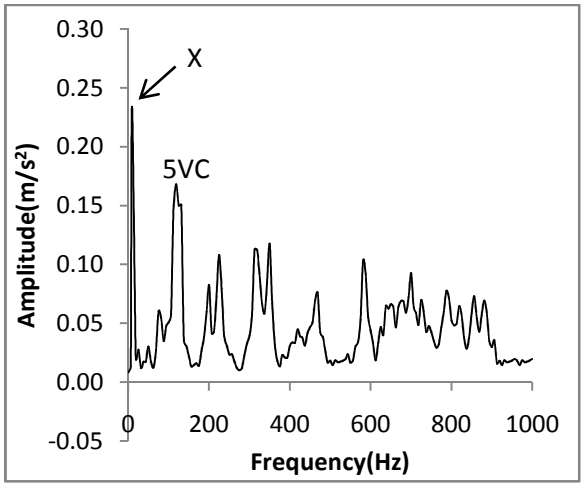

Figure 4.13 Response of bent shaft at 500 rpm

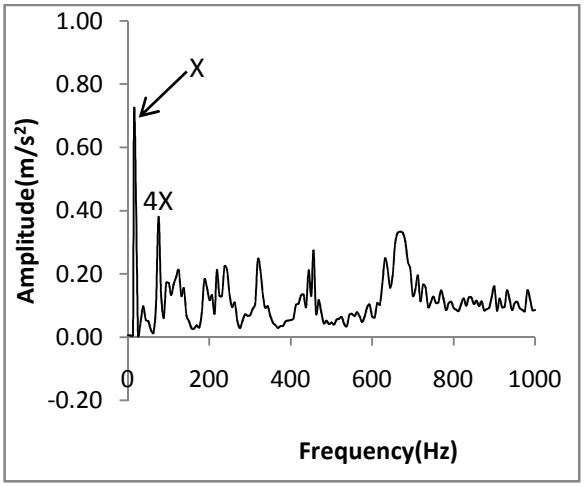

Figure 4.14 Response of bent shaft at 1000 rpm

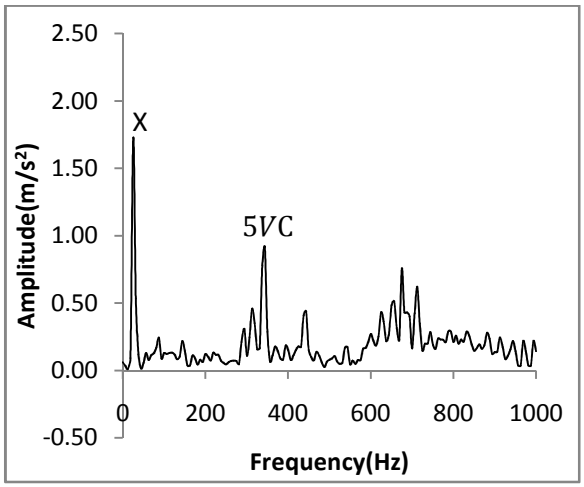

Figure 4.15 Response of bent shaft at 1500 rpm

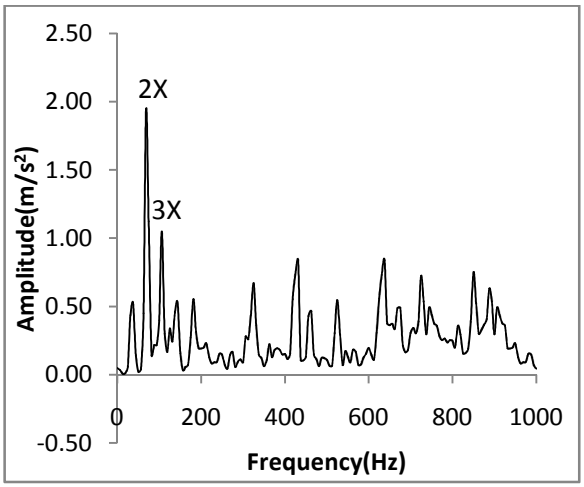

Figure 4.16 Response of bent shaft at 2000 rpm

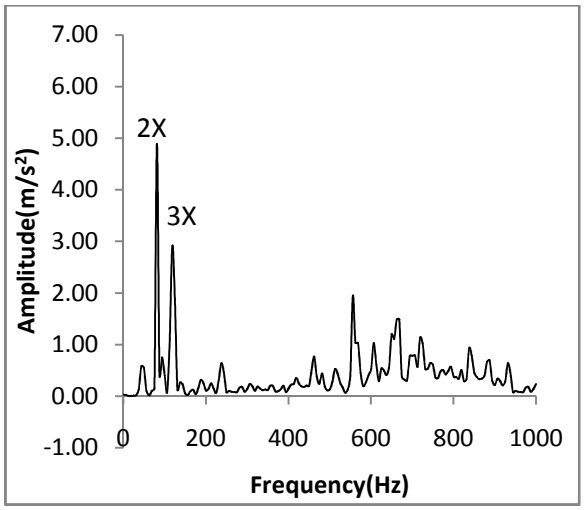

Figure 4.17 Response of bent shaft at 2500 rpm

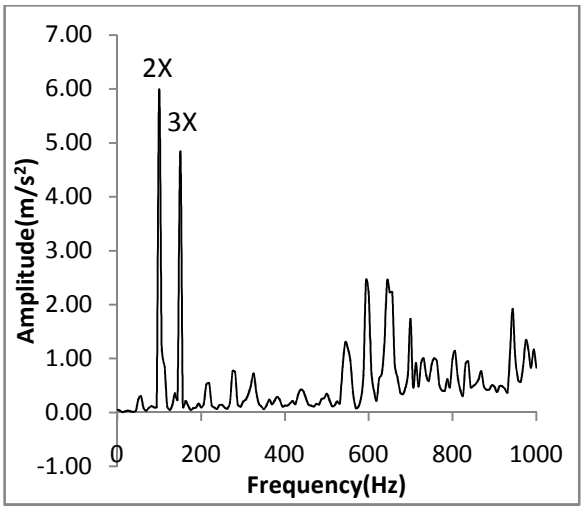

Figure 4.18 Response of bent shaft at 3000 rpm

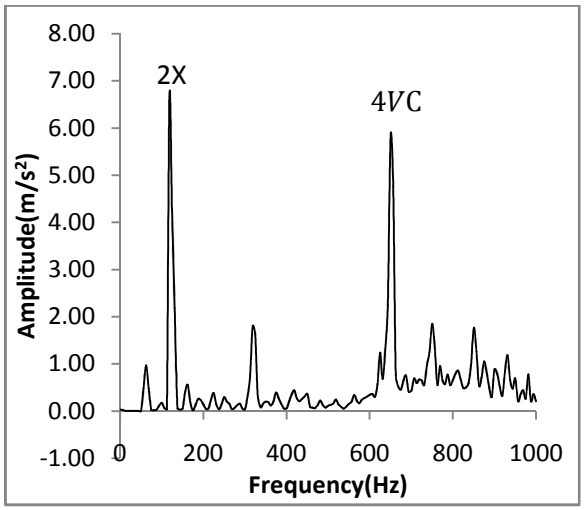

Figure 4.19 Response of bent shaft at 3500 rpm

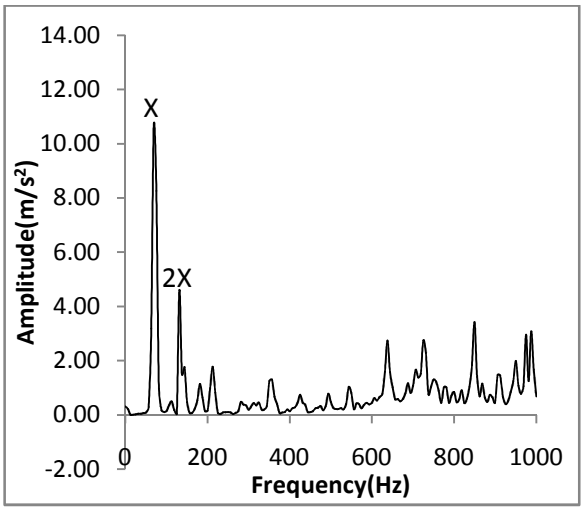

Figure 4.20 Response of bent shaft at 4000 rpm

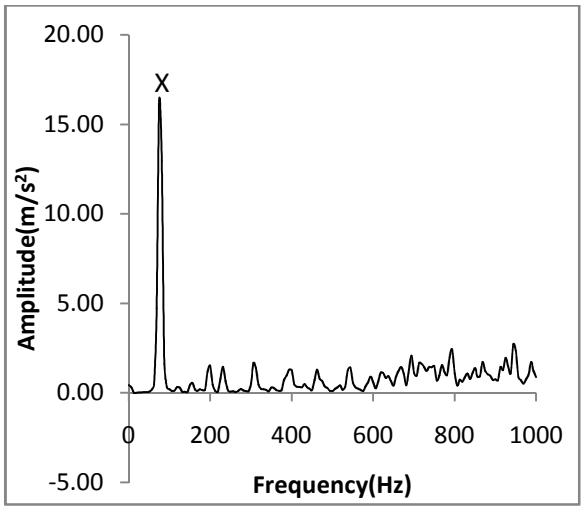

Figure 4.21 Response of bent shaft at 4500 rpm

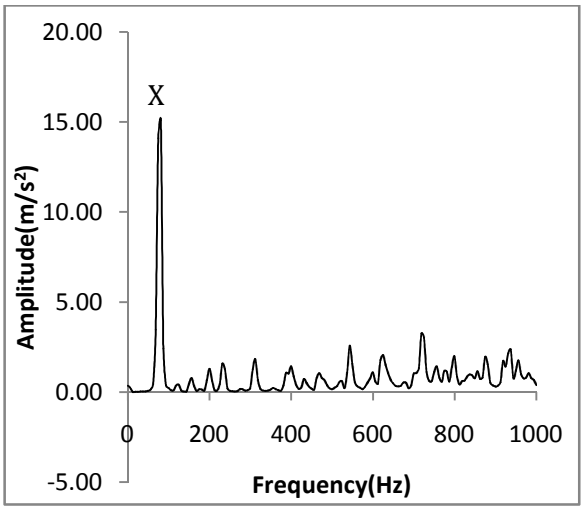

Figure 4.22 Response of bent shaft at 5000 rpm

Table 4.3 Summary of bent shaft

Speed (rpm)	Peak Amplitude	Harmonic in the shaft spectrum	Peak Amplitude Value (m/s^2)
500	*X*	5*VC*	0.234
1000	*X*	4*X*	0.725
1500	*X*	5*VC*	1.73
2000	2*X*	3*X*	1.94
2500	2*X*	3*X*	4.89
3000	2*X*	3*X*	5.99
3500	2*X*	4*VC*	6.67
4000	*X*	2*X*	10.7
4500	*X*	-	16.3
5000	*X*	-	15.1

4.3.1.3 Response of axial misaligned shaft (misaligned with motor shaft)

The vibration response at various speeds for the misaligned shaft is shown below from Figure 4.23 to 4.32. The value of amplitudes of misaligned shaft as compared to healthy shaft are more. The misalignment of the shaft is with the motor shaft and misalignment is of the dimension of 3mm. Figure 4.23 shows the response at 500 rpm which gives the peak values on rotational frequency (3*X*=24.99 Hz) and varying compliance frequency (*VC*=107.1 Hz). The vibrational plots in Figure 4.24 and 4.25 show the frequencies at 1000 and 1500 rpm respectively, in which peak amplitudes appear on multiple of the rotational frequency (3*X*=50.1 Hz, 7*X*=116.9 Hz) and (3*X*=75 Hz, 5*X*=125 Hz) respectively. The frequency spectra at 2000 rpm is shown in Figure 4.26, it is clear that peak values comes out on rotational frequency (3*X*=99.9 Hz) and varying compliance frequency (5*VC*=430.5 Hz). Figures 4.27 and 4.28 depict the result at 2500 rpm and 3000 rpm and it is clear that for 2500 rpm peaks appear on rotational frequencies (2*X*=83.4 Hz, 3*X*=125.1 Hz) and for 3000 rpm at (2*X*=100 Hz, 5*X*=250 Hz). At 3500 rpm response values are on rotational frequencies (*X*=58.3 Hz, 2*X*=116.6 Hz) and varying compliance

frequency (4VC=602.2 Hz). Plots of the Figure 4.30 at 4000 rpm and 4.31 at 4500 rpm have the peak values on rotational frequency(X=66.7 Hz, 4X=266.8 Hz) and (X=75 Hz) respectively. The value of amplitude at the speed of 5000 rpm appears on rotational frequency (X=83.3 Hz) and varying compliance frequency (2VC=428.4 Hz). Table 4.4 shows the summary of misaligned shaft at various speeds.

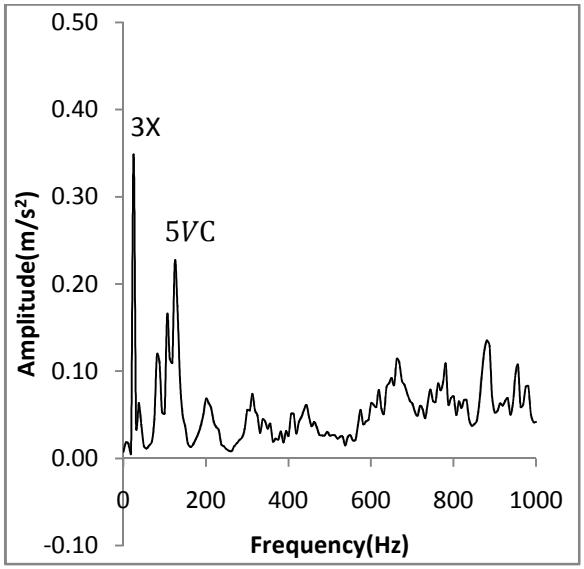

Figure 4.23 Response of misaligned shaft at 500 rpm

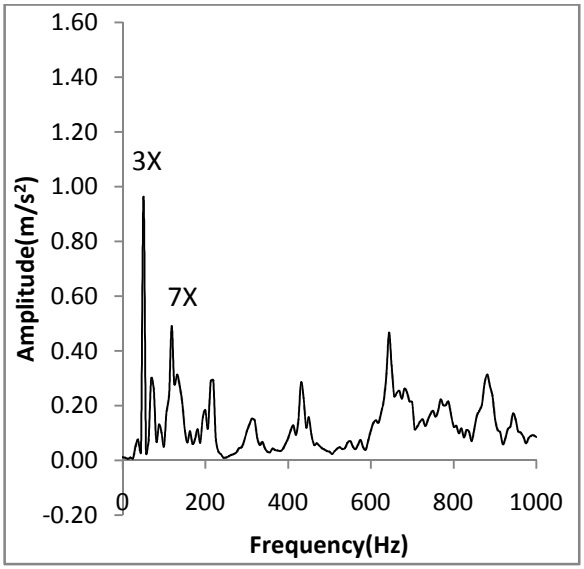

Figure 4.24 Response of misaligned shaft at 1000 rpm

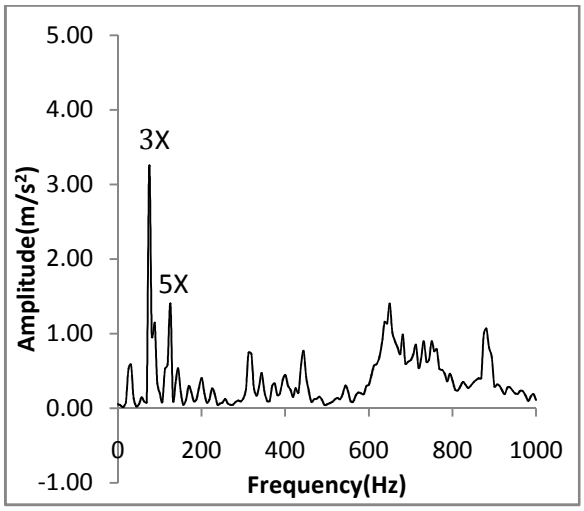

Figure 4.25 Response of misaligned shaft at 1500 rpm

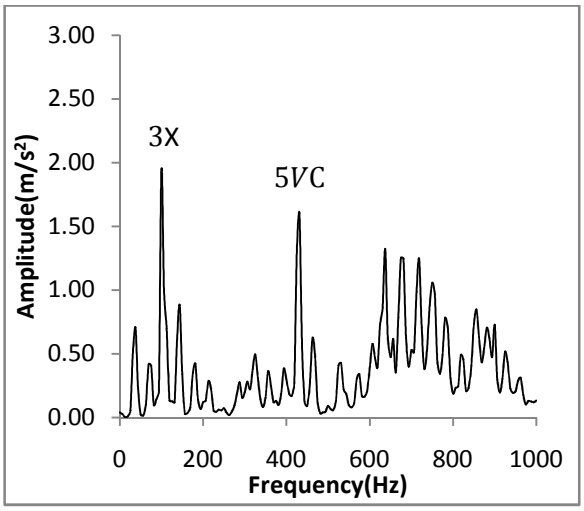

Figure 4.26 Response of misaligned shaft at 2000 rpm

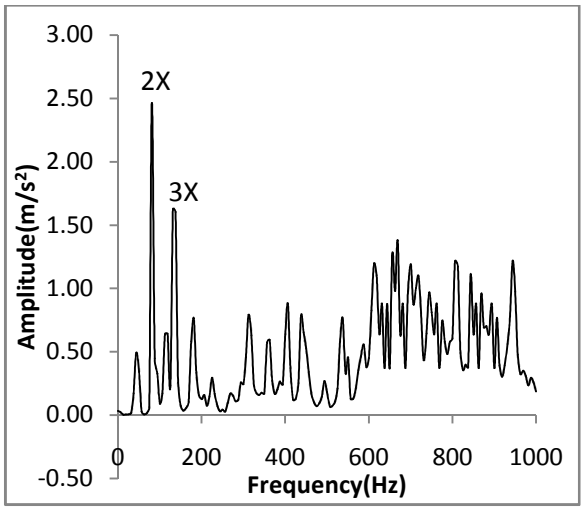

Figure 4.27 Response of misaligned shaft at 2500 rpm

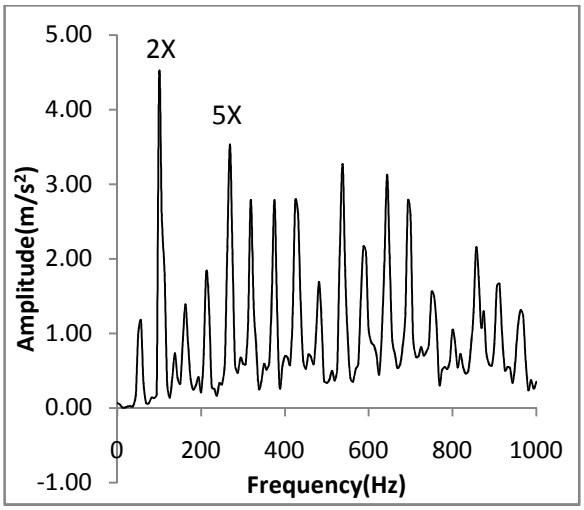

Figure 4.28 Response of misaligned shaft at 3000 rpm

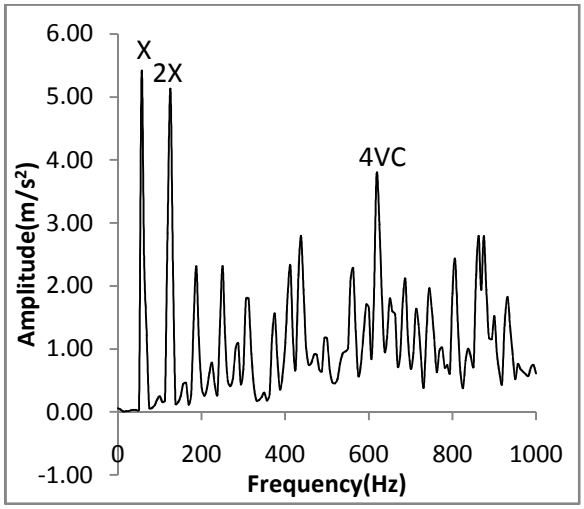

Figure 4.29 Response of misaligned shaft at 3500 rpm

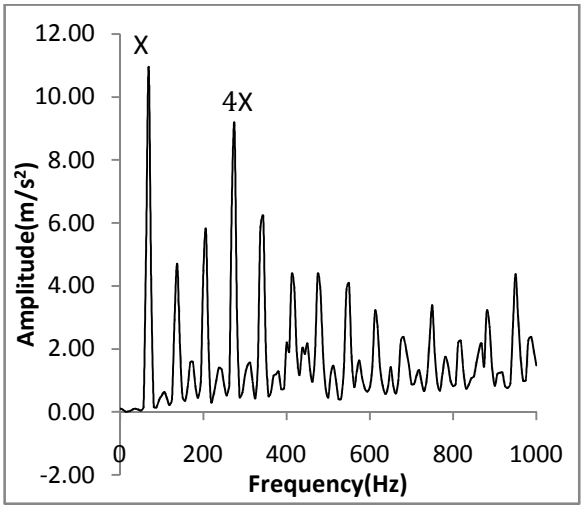

Figure 4.30 Response of misaligned shaft at 4000 rpm

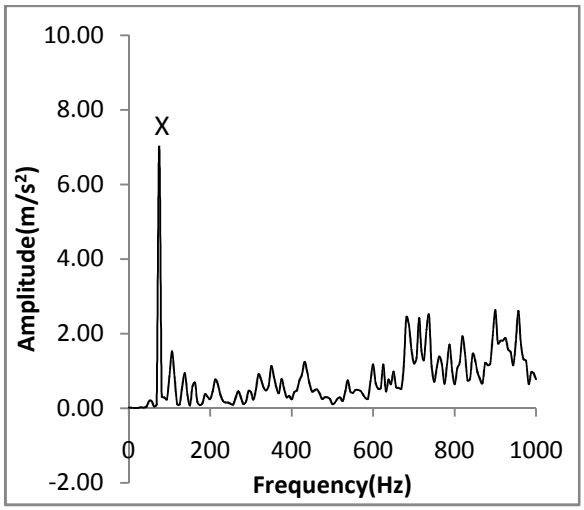

Figure 4.31 Response of misaligned shaft at 4500 rpm

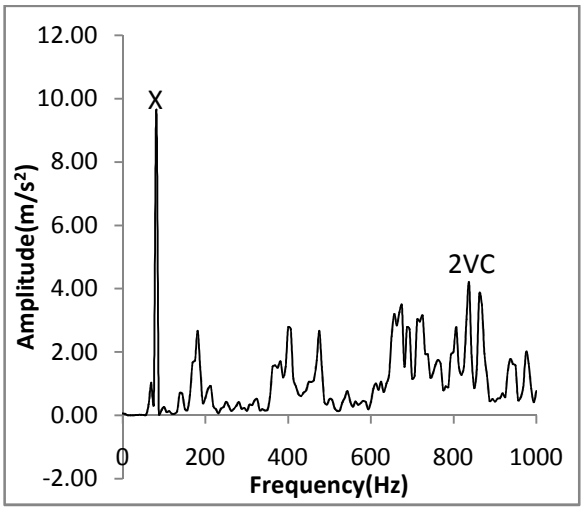

Figure 4.32 Response of misaligned shaft at 5000 rpm

Table 4.4 Summary of misaligned shaft

Speed (rpm)	Peak Amplitude	Harmonic in the shaft spectrum	Peak Amplitude Value (m/s^2)
500	3*X*	5*VC*	0.349
1000	3*X*	7*X*	0.963
1500	3*X*	5*X*	3.25
2000	3*X*	5*VC*	1.94
2500	2*X*	3*X*	2.46
3000	2*X*	5*X*	2.58
3500	*X*	2*X*, 4*VC*	5.38
4000	*X*	4*X*	11
4500	*X*	-	7.01
5000	*X*	2*VC*	9.65

4.3.1.4) Response of shaft having transverse crack (20% of diameter of shaft)

The vibration responses for the shaft having a transverse Crack of 20% of the diameter of shaft i.e. 4mm are shown below on the different speeds. As shown in the Figures the amplitude of vibration increases with increase in speed. Figure 4.33 shows the peak value at 500 rpm comes on sub-critical frequency and varying compliance frequency ((1/3) ω_c=36.72 Hz) and (6*VC*=128.52 Hz). Figure 4.34 gives the response values at 1000 rpm which shows the peak values on sub-critical frequency and multiple of rotational frequency ((1/2)ω_c =55.1Hz) and (5*X*=83.5 Hz). The peak in the vibration spectrum for the speed of 1500 rpm shown in Figure 4.35 is on critical frequency of the shaft and varying compliance frequency (ω_c=110.16 Hz) and (5*VC*=321.65 Hz). The results at 2000 rpm in Figure 4.36 and 2500 rpm in Figure 4.37 clearly appears on rotational frequency (*X*=33.3 Hz), critical frequency of shaft (ω_c=110.16 Hz) and varying compliance frequency (6*VC*=642.6 Hz). Figure 4.38 demonstrate the peak values for the speed of 3000 rpm. It is clear that the amplitude appear on rotational frequency and its multiple (2*X*=100 Hz) and

(13*X*=650 Hz). Vibration spectrum at 3500 rpm is given in Figure 4.39, which shows that peak appear on the sub-harmonic of critical frequency ((1/2)ω_c=55.1Hz). The value of amplitude at 4000 rpm in Figure 4.40 and at 4500 rpm in Figure 4.41 comes on rotational frequency and varying compliance frequency (*X*=66.7 Hz, 4*VC*=686 Hz) and (*X*=75 Hz, 5*VC*=966 Hz) respectively. Now when the speed of the shaft is 5000 rpm then the peak values are on rotational frequency (*X*=83.3 Hz, 5*X*=416.5 Hz) and varying compliance frequency (4*VC*=856.8 Hz). The summary for shaft having Transverse crack at different RPMs is shown in Table 4.5.

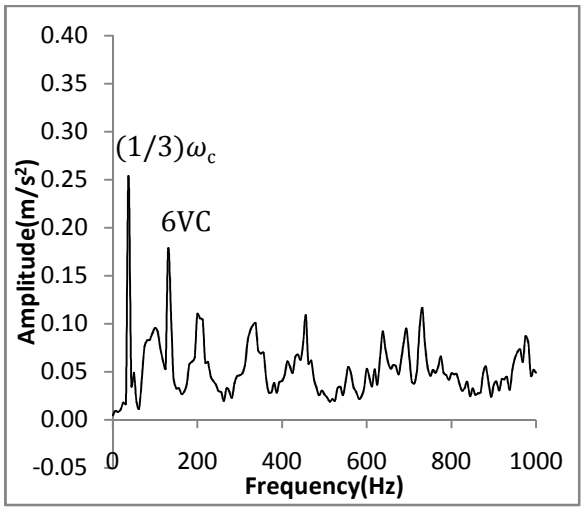

Figure 4.33 Response of shaft having transverse crack at 500 rpm

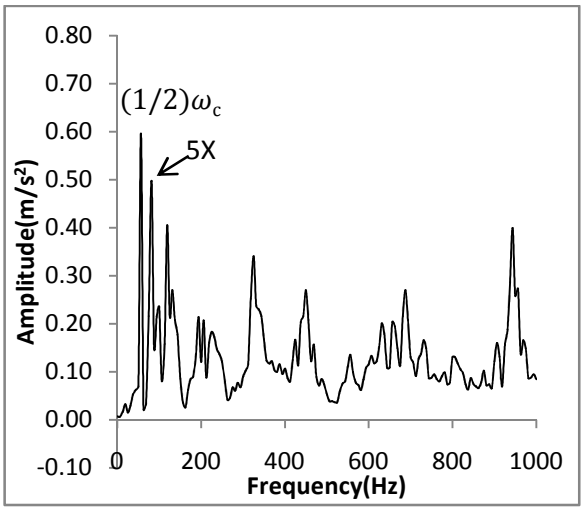

Figure 4.34 Response of shaft having transverse crack at 1000 rpm

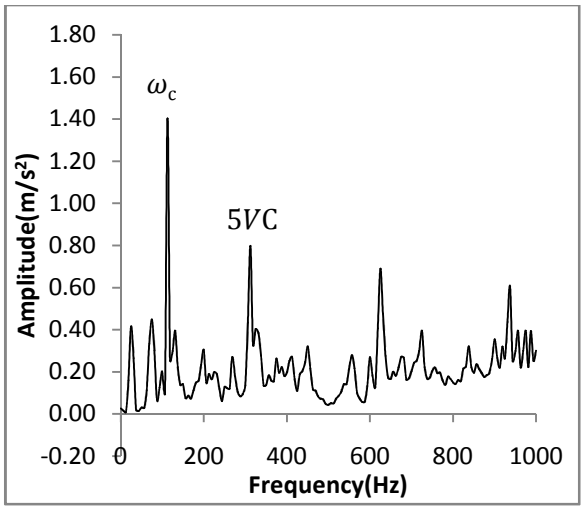

Figure 4.35 Response of shaft having transverse crack at 1500 rpm

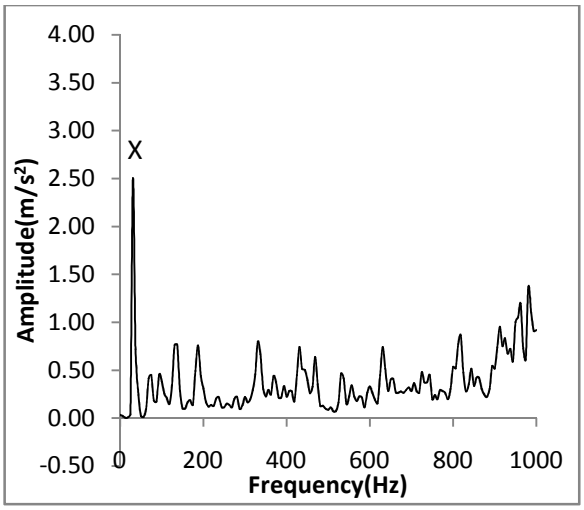

Figure 4.36 Response of shaft having transverse crack at 2000 rpm

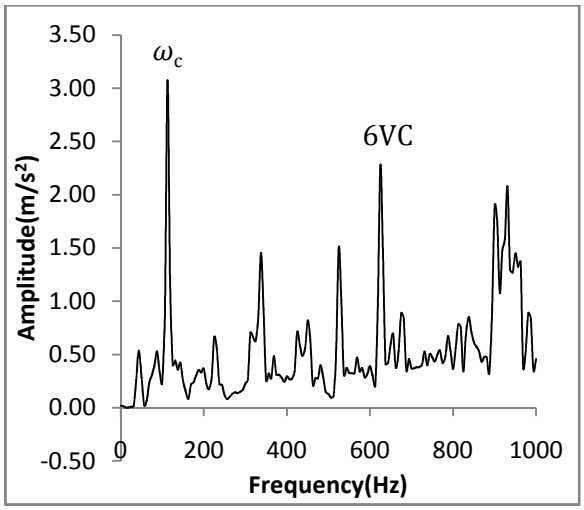

Figure 4.37 Response of shaft having transverse crack at 2500 rpm

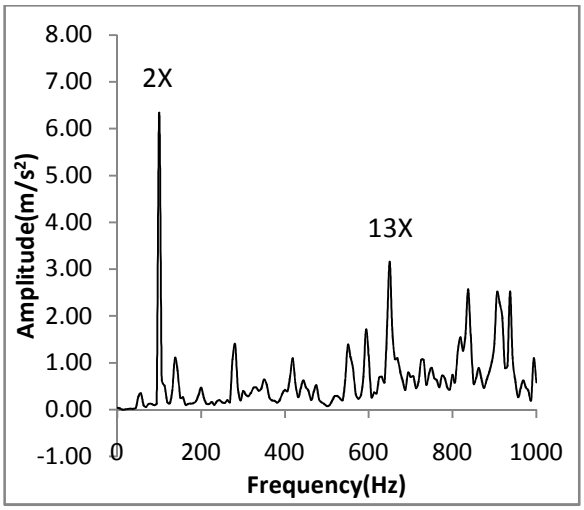

Figure 4.38 Response of shaft having transverse crack at 3000 rpm

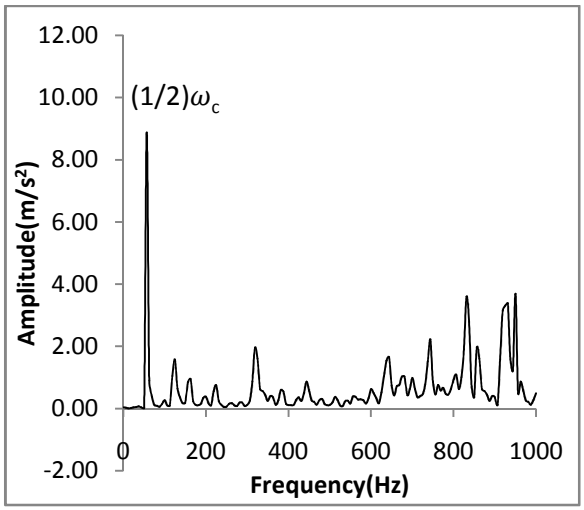

Figure 4.39 Response of shaft having transverse crack at 3500 rpm

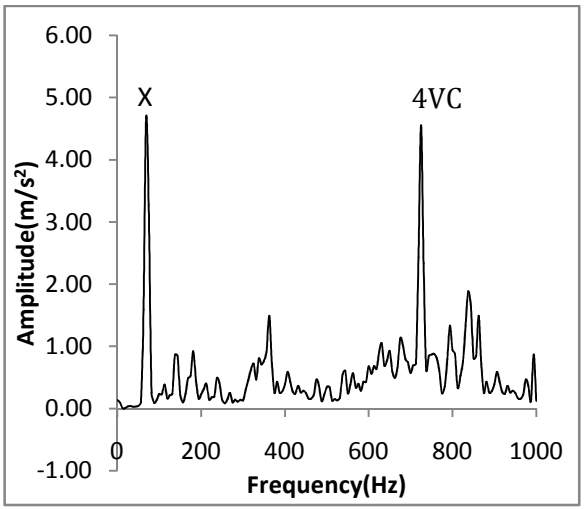

Figure 4.40 Response of shaft having transverse crack at 4000 rpm

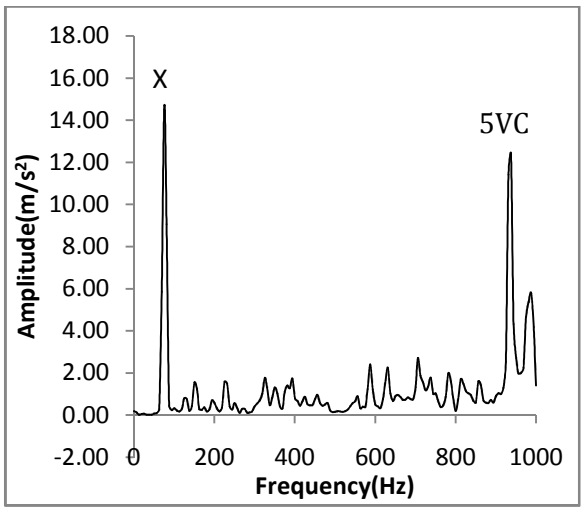

Figure 4.41 Response of shaft having transverse crack at 4500 rpm

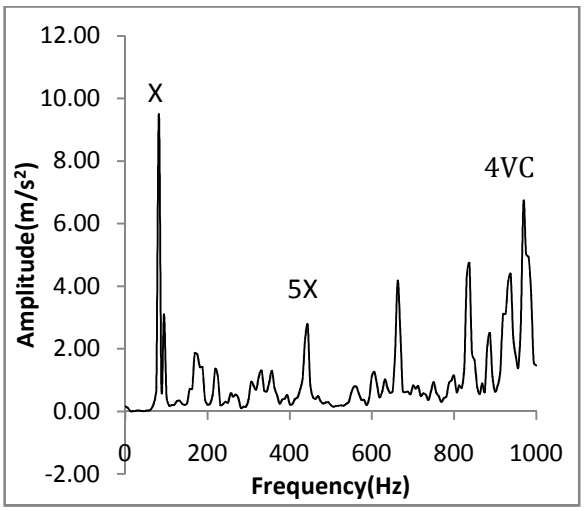

Figure 4.42 Response of shaft having transverse crack at 5000 rpm

Table 4.5 Summary of shaft having transverse crack

Speed (rpm)	Peak Amplitude	Harmonic in the shaft spectrum	Peak Amplitude Value (m/s^2)
500	$(1/3)\omega_c$	$6VC$	0.254
1000	$(1/2)\omega_c$	$5X$	0.596
1500	ω_c	$5VC$	1.4
2000	X	-	2.5
2500	ω_c	$6VC$	3.07
3000	$2X$	$13X$	6.34
3500	$(1/2)\omega_c$	-	8.87
4000	X	$4VC$	4.66
4500	X	$5VC$	14.7
5000	X	$5X$, $4VC$	9.49

4.3.1.5) Response of shaft having slant crack of 45° (20% of diameter of shaft)

The vibration responses at the different speeds for the shaft having a slant crack which is of 20% of the diameter of shaft are shown in the graphs below. The angle of the crack is 45° and depth is 4mm. As compared to transverse crack the values of the peak amplitudes are lesser in case of Slant crack. Figure 4.43 at 500 rpm shows the peak value in the vibration spectrum on sub-harmonic ($(1/2)\omega_c$ =55.1Hz) and super-harmonic of the critical frequency ($3\omega_c$=330.48 Hz). The vibration response at 1000 rpm as given in Figure 4.44, clearly shows the apex value on the rotational frequency (X=16.67 Hz) and super-harmonic of critical frequency ($2\omega_c$=220.32 Hz). The response values at 1500 rpm and 2000 rpm comes on rotational frequencies and varying compliance frequencies ($2X$=100 Hz, $2VC$=128.66 Hz) and (X=33.3 Hz, $5VC$=430.5 Hz) respectively. At 2500 rpm as shown in Figure 4.47 peak in the vibration spectrum is on one-half of the critical frequency ($(1/2)\omega_c$ =55.1Hz) and multiple of varying compliance frequency ($5VC$=535.5 Hz). In Figure 4.48, vibration spectra for 3000 rpm is given, which clearly shows the spike

on the critical frequency of the shaft (ω_c=110.16 Hz). The result at the speed of 3500 rpm shows the apex value on sub-critical frequency ((1/2)ω_c =55.1Hz), rotational frequency (2*X*=116.6 Hz) and varying compliance frequency (6*VC*=898.8 Hz). Apex values at 4000 rpm are on rotational frequency (*X*=66.7 Hz, 2*X*=133.4 Hz). The vibration response, as shown in the Figure 4.51 at 4500 rpm and Figure 4.52 at 5000 rpm, clearly shows the peak values on rotational frequency and varying compliance frequency (*X*=75 Hz, 4*VC*=772.8 Hz) and (*X*=83.3 Hz, 3*VC*=642.6 Hz) respectively. The summary of the shaft having slant crack at various speeds is given in Table 4.6.

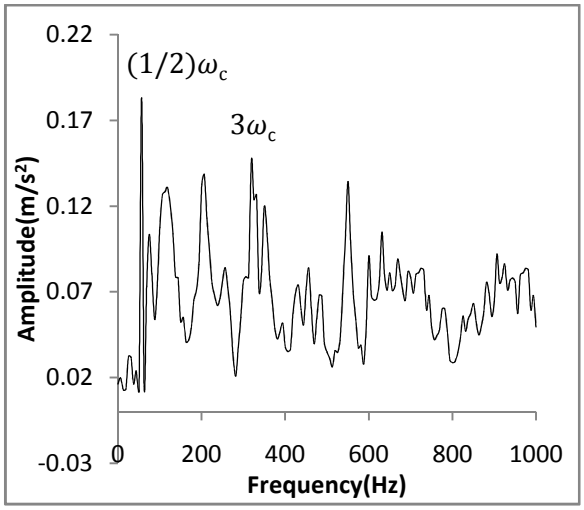

Figure 4.43 Response of shaft having slant crack at 500 rpm

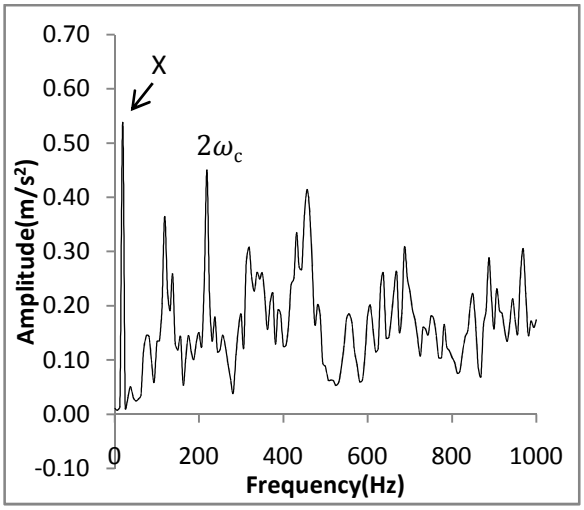

Figure 4.44 Response of shaft having slant crack at 1000 rpm

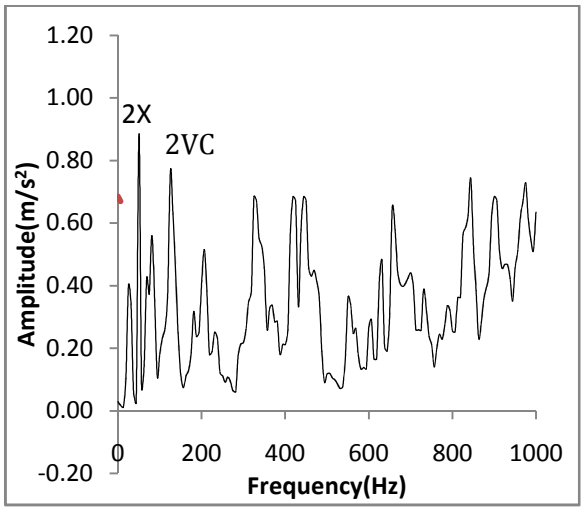

Figure 4.45 Response of shaft having slant crack at 1500 rpm

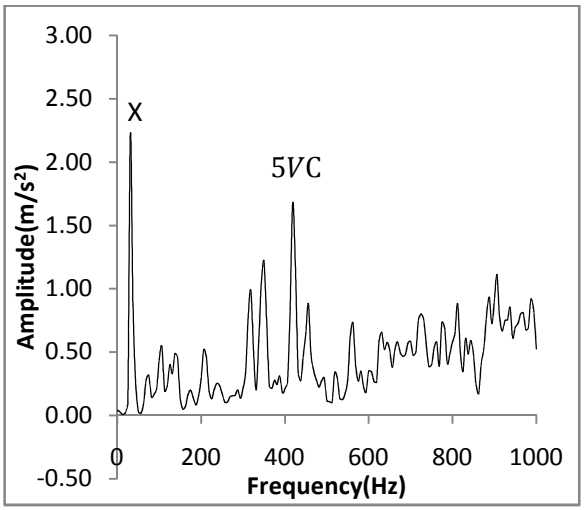

Figure 4.46 Response of shaft having slant crack at 2000 rpm

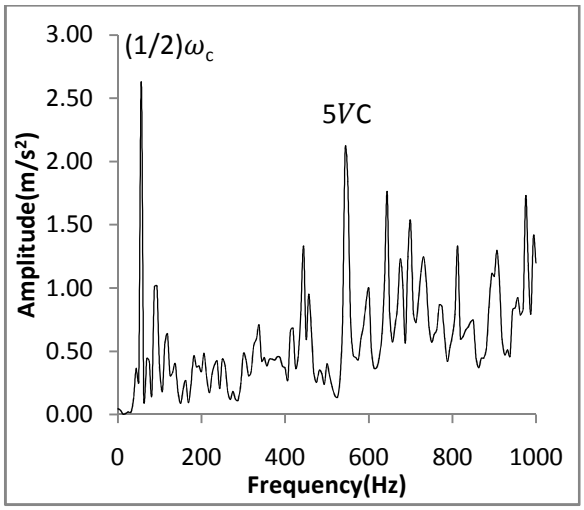

Figure 4.47 Response of shaft having slant crack at 2500 rpm

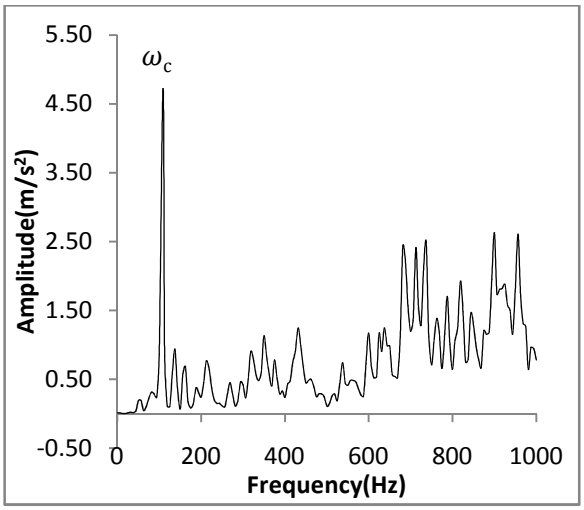

Figure 4.48 Response of shaft having slant crack at 1000 rpm

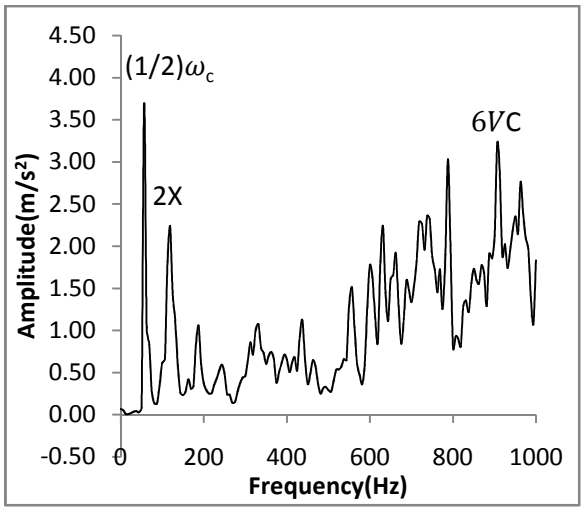

Figure 4.49 Response of shaft having slant crack at 3500 rpm

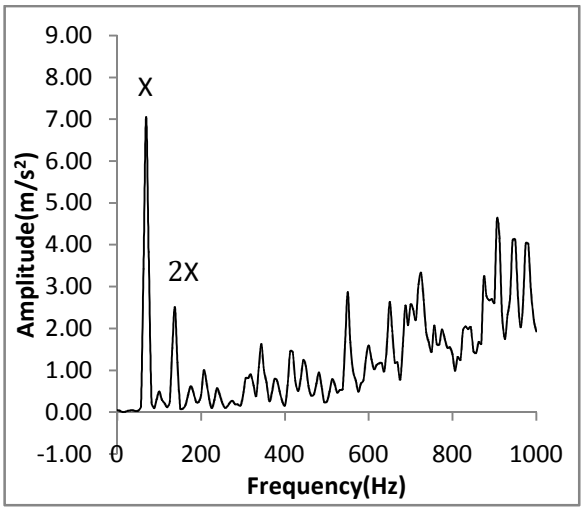

Figure 4.50 Response of shaft having slant crack at 4000 rpm

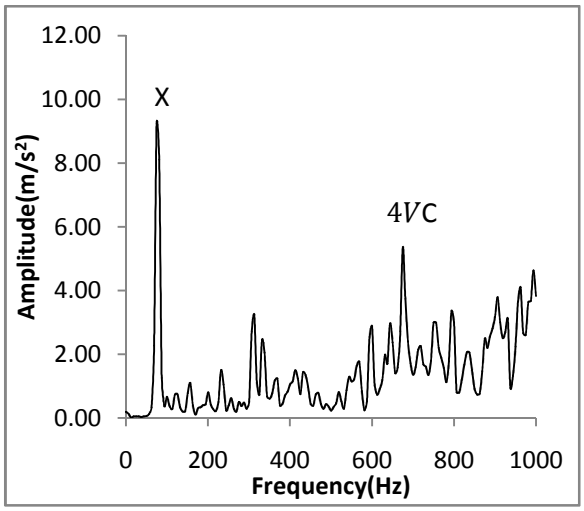

Figure 4.51 Response of shaft having slant crack at 4500 rpm

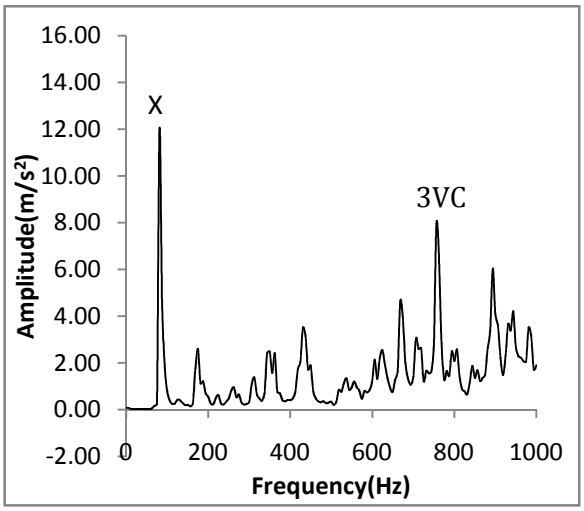

Figure 4.52 Response of shaft having slant crack at 5000 rpm

Table 4.6 Summary of shaft having slant crack

Speed (rpm)	Peak Amplitude	Harmonic in the shaft spectrum	Peak Amplitude Value (m/s^2)
500	$(1/2)\omega_c$	$3\omega_c$	0.183
1000	X	$2\omega_c$	0.538
1500	$2X$	$2VC$	0.886
2000	X	$5VC$	2.22
2500	$(1/2)\omega_c$	$5VC$	2.63
3000	ω_c	-	4.72
3500	$(1/2)\omega_c$	$2X$, $6VC$	3.69
4000	X	$2X$	7.05
4500	X	$4VC$	9.23
5000	X	$3VC$	12.01

4.4 STUDY OF FAULTS OF ROTOR BEARING SYSTEM USING RESPONSE SURFACE METHODOLOGY (RSM)

The presence of faults in the rotor bearing system result in increased vibrations. Rotor speed also has an important role in vibrations of shaft. The interaction between the different type of defects and speed helps to study their effect on vibrations more effectively. Response surface methodology (RSM) is a combination of statistical and mathematical techniques to represent the relationship between the inputs and the outputs of a physical system. In general, RSM established the methods for drawing inferences from observations, when inferences are not exact but subject to variation. There is very less work has been reported in the literature related to its application in predicting of vibration associated with faults in shafts. Recently, RSM has been used for study the effect of various factors and their interactions with the development of response surface models in dynamic analysis of bearings (Gallina et al., 2006; Liang et al., 2007). The proposed study uses RSM to study the influence of faults in shaft and speed on vibrations

of the rotor bearing system. Vibration amplitude is used as a response factor. Experiments are performed using 6304 ball bearings and EN8 steel shaft with various conditions.

In this study, effect of various defects in shafts on the vibration response of a rotor bearing system has been analyzed using RSM. Interaction between different faults and rotor speed is also studied using RSM. Severe vibration conditions are determined by approximating amplitude of vibration using a series of polynomials using RSM. Defects in the shafts are considered as bent shaft, misalignment, transverse crack and slant crack. Experiments have been carried out for healthy and defective shafts at various speeds. Vibration responses for all cases are presented in form of FFT.

4.4.1 Response Surface Methodology

Response surface methodology establishes the methods for drawing inferences from observations, when inferences are not exact but subject to variation. The response surface methodology is a collection of mathematical and statistical techniques that are useful for modeling and analysis in applications, where a response interest is influenced by several variables (factors) and the objective is to optimize this response. It is not necessary that the response is affected by a single factor at a time and there is many situations in which one or more factors affect response simultaneously. So, it is necessary to study the interaction (dependence) between the factors when the effect of one factor depends on the behaviour of another. The application of the RSM becomes crucial when it is necessary to explore the relationship between the factors and response (dependent) variable within the experimental region and not only at the boundaries. RSM has been developed by Box and Wilson (1951) to explore the potential of statistical design in industrial experiments. This methodology has been found extensive application in a wide variety of industrial settings like chemical processes, semiconductor and electronics manufacturing, machining, metal cutting, and joining processes etc . RSM constructs polynomial approximations to build functional relationships between design variables and performances (Myers and Montgomery, 1995). The input variables are sometimes called independent variables or factors, and the performance measures or quality characteristics are called as responses. For the most response surface, the relationship between the response variable of interest (y_0) and the factors ($x_1, x_2, \ldots, x_k$) may be described in the following second-order equation.

$$y_0 = f(x_0) = \beta_o + \sum_{i=1}^{n} \beta_i x_i + \sum_{i=1}^{n} \beta_{ii} x^2{}_i + \sum_{i=1, j>1}^{n} \beta_{ij} x_i x_j + \varepsilon \qquad (4.3)$$

Where ε represents the noise or error observed in the response y_0, β_0, β_i … are polynomial coefficients and n is number of factors. Eq. (4.3) can also be expressed in matrix form as

$$Y_0 = X_0 B + \varepsilon \tag{4.4}$$

The method of least squares is used to estimate the polynomial coefficients in approximating polynomials such that minimize the sum of squares of the model errors. Then matrix B of polynomial coefficients can be obtained from the formula

$$B = \left(X_0{}^T X_0\right)^{-1} X_0{}^T Y_0 \tag{4.5}$$

The response surface analysis is done in terms of the fitted surface. Analysis of variance (ANOVA) is used to check the fitness of the model once a response surface model is obtained.

4.4.2 Experimentation

Shafts are of paramount importance to almost all forms of rotating machinery. Predicting the severe vibration conditions due to defects in shafts is extremely important in industries. In the present work, a simple test equipage as shown in Figure 4.1 is used with rotor supported on SKF 6304 ball bearings. Various parameters of shafts used for the study are listed in Table 4.7.

In the present study, experiments are carried out to analyze effect of various shaft defects on the vibration response of the rotor bearing system using response surface method. As a first step, the machine operated with healthy shaft in healthy ball bearings to establish the base-line data. Then data is collected for different defective conditions. A variety of defects are simulated on the equipage at 1000 rpm, 2500 rpm and 5000 rpm. In order to perform response surface analysis to determine the combination of defects that gives the severe vibration conditions, DOE is used with total 21 trial runs. Table 4.8 shows parameters used for DOE with their minimum and maximum level.

4.4.2.1 Types of defects in shafts

1) Bent Shaft
2) Misaligned Shaft
3) Transverse Crack
4) Slant Crack (45°)

(a) **(b)**

Figure 4.53 (a) Transverse Crack (b) Slant Crack

Table 4.7 Parameters of shafts used for experiment

Parameter	Value
Material of shaft	EN8 steel
Weight	2.5 Kg
Length	760mm
Diameter	21mm

Table 4.8 Parameters for DOE

Parameter Designation Symbols	Parameters	Minimum Level	Maximum Level
A	Bent Shaft	0	3 mm
B	Misaligned shaft	0	3 mm
C	Transverse Crack	0	4 mm
D	Slant Crack	0	4mm
E	Speed	1000 rpm	5000 rpm

4.4.2.2 Response surface model establishment

In order to predict vibration amplitudes using RSM, first various factors affecting amplitude of vibrations and stability of the rotor are identified. For this study, the factors that are of interest are various defect conditions in shaft and shaft speed which are given below:

(1) Bent Shaft

(2) Misaligned Shaft

(3) Transverse Crack (Figure 4.53 a)

(4) Slant Crack (45°) (Figure 4.53 b)

(5) Shaft Speed

Three levels of each of these factors are selected. The maximum and minimum levels of each factor are defined in Table 4.8. In order to perform DOE to determine the condition that gives the severe vibration conditions, experiments are carried out in 21 trials listed in Table 4.9.

Table 4.9 DOE Set and Results

	Bent shaft (mm)	**Misaligned Shaft (mm)**	**Transverse Crack (mm)**	**Slant Crack (mm)**	**Shaft Speed (rpm)**	**Vibration response (Peak Amplitude) (m/s^2)**
Trial	**A**	**B**	**C**	**D**	**E**	**R1**
1	0	0	0	0	1000	0.3894
2	3	0	0	0	1000	0.725
3	0	3	0	0	1000	0.963
4	0	0	2	0	1000	0.4698
5	0	0	4	0	1000	0.596
6	0	0	0	2	1000	0.601
7	0	0	0	4	1000	0.538
8	0	0	0	0	2500	1.962
9	3	0	0	0	2500	4.89
10	0	3	0	0	2500	2.462
11	0	0	2	0	2500	1.647
12	0	0	4	0	2500	3.074
13	0	0	0	2	2500	1.727
14	0	0	0	4	2500	2.629
15	0	0	0	0	5000	8.16
16	3	0	0	0	5000	15.09
17	0	3	0	0	5000	9.650
18	0	0	2	0	5000	10.24
19	0	0	4	0	5000	9.49
20	0	0	0	2	5000	5.29
21	0	0	0	4	5000	12.01

4.4.3 Results and Discussion

The vibration response plots for healthy and defective shafts at 1000, 2500 and 5000 rpm are shown in form of frequency spectra.

Figure 4.54 to 4.60 shows the vibration response at 1000 rpm. Figure 4.54 gives the results of healthy shaft; it is clear that the peak value falls on critical frequency of the shaft (ω_c) and at interaction of rotational frequency and varying compliance frequency ($6X+5VC$). The response for the bent shaft in Figure 4.55 and misaligned shaft in Figure 4.56 at 1000 rpm comes on rotational frequency and its multiple(X, $4X$) and ($3X$, $7X$). The nature of solution for transverse crack (2mm) and slant crack (2mm) are shown in the Figure 4.57 and Figure 4.58 respectively which depict the response on sub-harmonic of critical frequencies and multiple of varying compliance frequencies ($(1/2)\omega_c$, $3VC$) and ($(1/2)\omega_c$, $10VC$). The results for transverse crack (4mm) shown in Figure 4.59 are at sub-harmonic of critical frequency ($(1/2)\omega_c$) and varying compliance frequency ($5X$) and for slant crack (4mm) in Figure 4.60 are at super-harmonic of critical frequency ($2\omega_c$) and rotational frequency (X).

The response plots for 2500 rpm are shown in the Figure 4.61 to 4.67. The peak values in the frequency spectrum for healthy shaft (Figure 4.61) appear on rotational frequency ($2X$) and varying compliance frequency ($6VC$). The apex value for bent shaft (Figure 4.62) and misaligned shaft (Figure 4.63) come out on rotational frequencies and on their multiples ($2X$, $3X$) and ($2X$, $3X$) respectively. Similarly for transverse crack (2mm) as shown in Figure 4.64 and slant crack (2mm) in Figure 4.65 appear on rotational frequency (X, $3X$), ($2X$) and on varying compliance frequency ($7VC$). The type of the solution for transverse crack (4mm) (Figure 4.66) is on critical frequency of the shaft (ω_c) and multiple of the varying compliance frequency. Slant crack (4mm) in Figure 4.67 gives the value on sub-harmonic of critical frequency ($(1/2)\omega_c$) and varying compliance frequency ($5VC$).

The vibration spectrum at 5000 rpm is given in the Figure 4.68 to 4.74. The response of healthy shaft given in Figure 4.68, appears on rotational frequency (X) and varying compliance frequency ($4VC$). The nature of the solution given in Figure 4.69 and Figure 4.70 tells about the bent shaft and misaligned shaft, which shows the peak values at rotational frequencies (X) and varying compliance frequency ($2VC$). Likewise transverse crack (2mm) in Figure 4.71 shows the result on rotational frequency (X). Figure 4.72 and 4.73 render the solution of slant crack (2mm) and transverse crack (4mm) which appear on rotational frequency and varying compliance frequency (X, $4VC$) and (X, $5X$, $4VC$). Slant

crack (4mm) shown in Figure 4.74 which depict the nature of solution on rotational frequency (X) and varying compliance frequency ($3VC$).

Table 4.9 shows for the trials 1 to 21 peak amplitude of vibration appears in the spectrum for acceleration response. Through the experiments, the polynomials *f(x)* is approximated by the design parameters (A, B, C, D and E). The final functions of response surface model are shown in Eq. (4.6), which is given below:
The approximated polynomial for horizontal acceleration response is;

$$\begin{aligned} \text{Amplitude} = {} & -0.16830 - 0.57076 \times \text{Bent Shaft} + 0.79663 \times \text{Misaligned Shaft} \\ & + 0.22072 \times \text{TransverseCrack} + 2.10857 \times \text{Slant Crack} \\ & - 2.02497\text{E-}004 \times \text{Speed} + 1.38026\text{E-}003 \times \text{Bent Shaft} \times \text{Speed} \\ & - 1.23715\text{E-}003 \times \text{Slant Crack} \times \text{Speed} - 0.55705 \times \text{Slant Crack}^2 \\ & + 4.00348\text{E-}007 \times \text{Speed}^2 + 3.52874\text{E-}004 \times \text{Slant Crack}^2 \times \text{Speed} \end{aligned} \quad (4.6)$$

The performance prediction of vibration amplitude response has been shown in Fig 4.75. The actual and predicted values of response are very close and verify fitness of polynomial for response.
In order to verify whether the obtained polynomials are valuable or not, the variance analysis and F-ratio test on them have been performed. Analysis of variance for acceleration response is shown in Table 4.10. The model F-value of 128.68 shows, the model is significant. Values of "Prob > F" less than 0.0500 indicate model terms are significant. In this case A, D, E, AE, DE, D^2, E^2 and D^2E are significant model terms. After testing the polynomials using ANOVA, these are used to analyze the relation between factors and their corresponding responses. Response surfaces for acceleration responses are developed as shown in Figures 4.76 to 4.85.

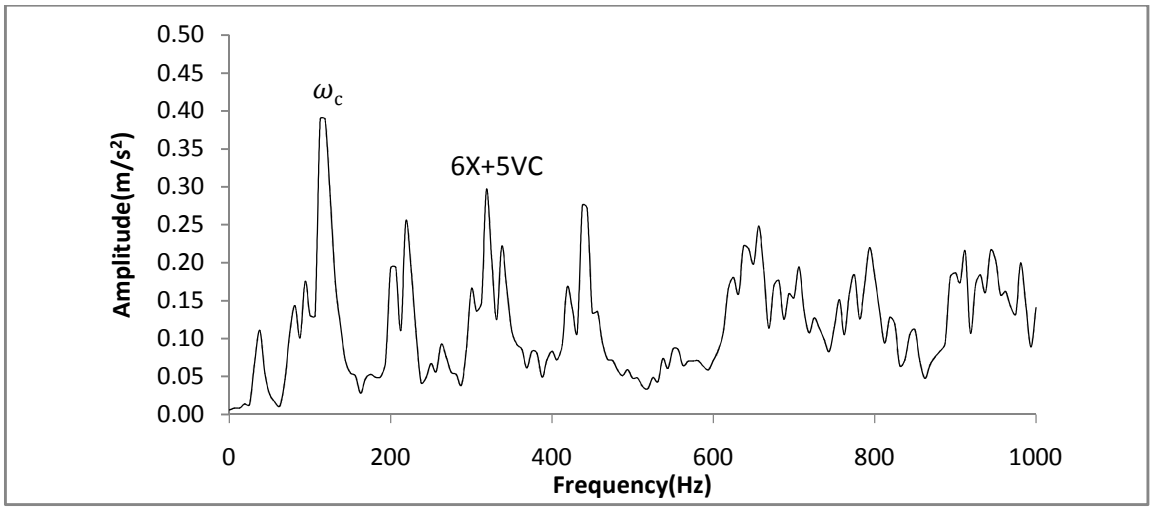

Figure 4.54 Response of healthy shaft at 1000 rpm

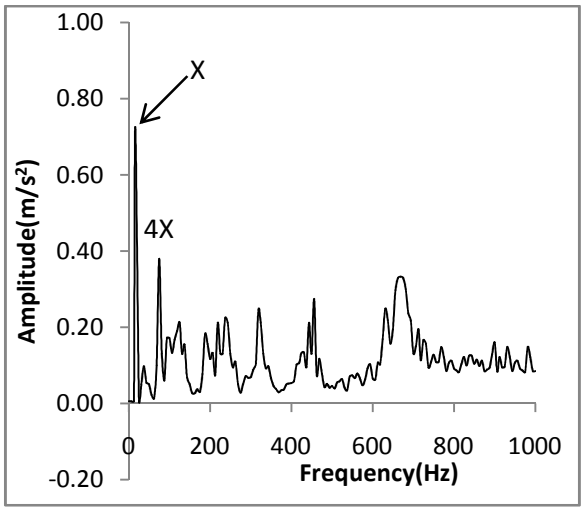

Figure 4.55 Response of bent shaft at 1000 rpm

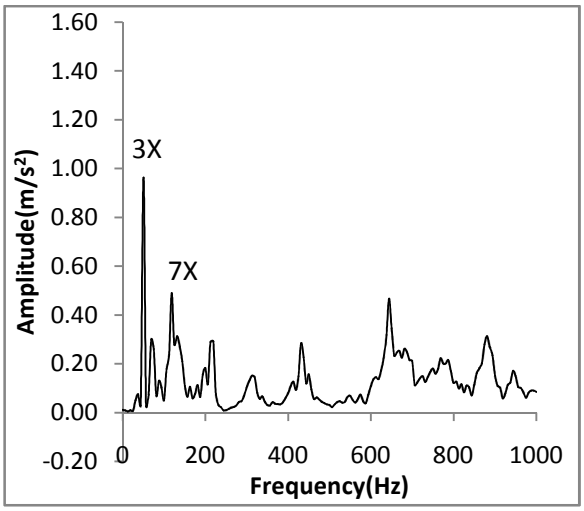

Figure 4.56 Response of misaligned shaft at 1000 rpm

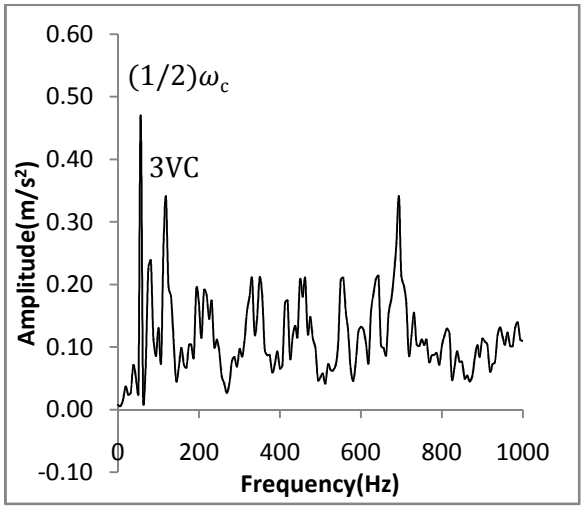

Figure 4.57 Response of transverse crack (2mm) at 1000 rpm

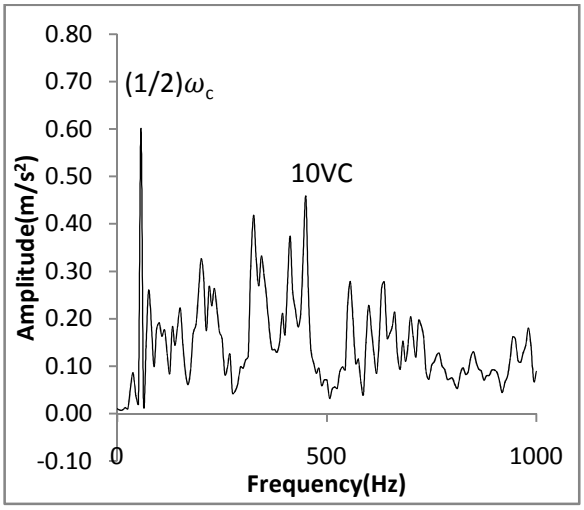

Figure 4.58 Response of slant crack (2mm) at 1000 rpm

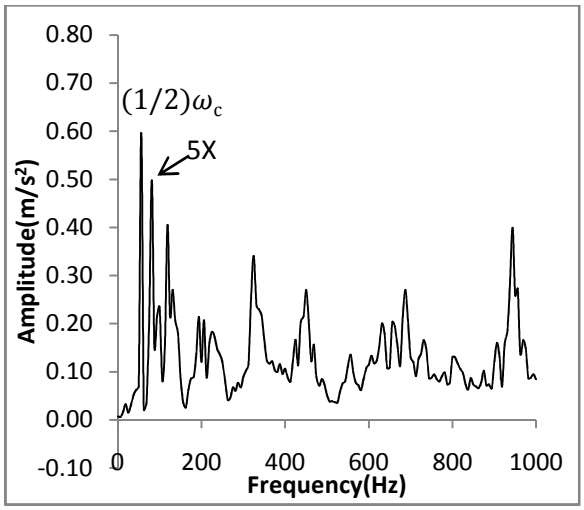

Figure 4.59 Response of transverse crack (4mm) at 1000 rpm

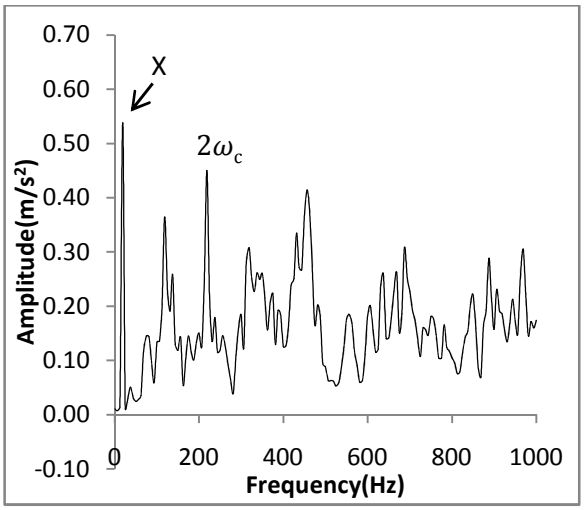

Figure 4.60 Response of slant crack (4mm) at 1000 rpm

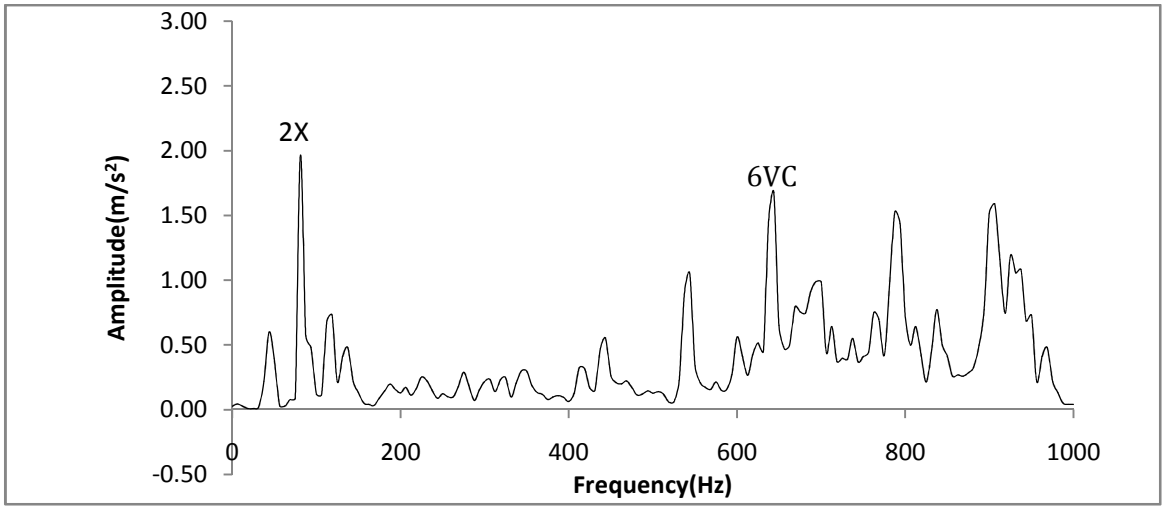

Figure 4.61 Response of healthy shaft at 2500 rpm

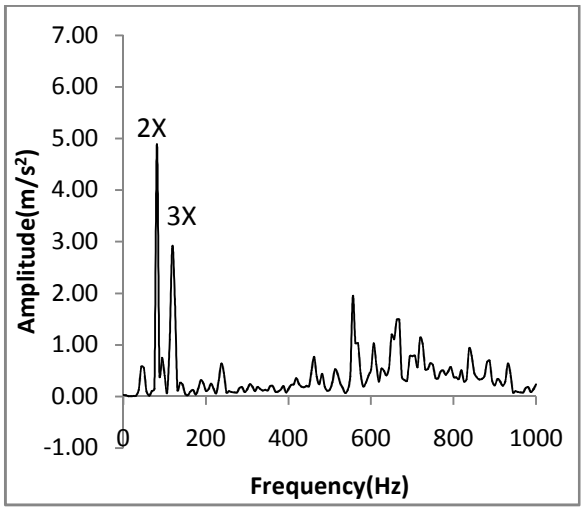

Figure 4.62 Response of bent shaft at 2500 rpm

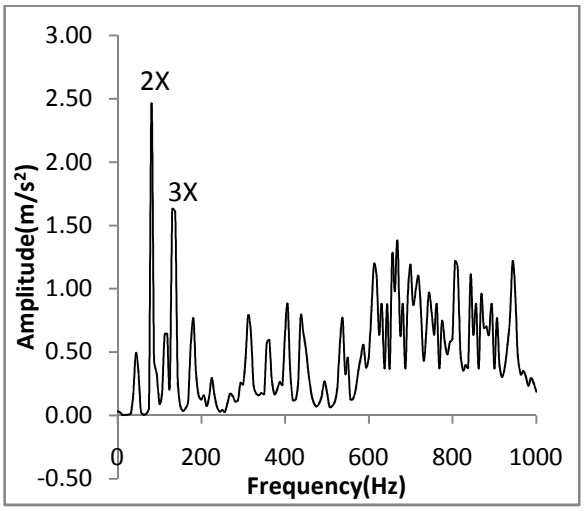

Figure 4.63 Response of misaligned shaft at 2500 rpm

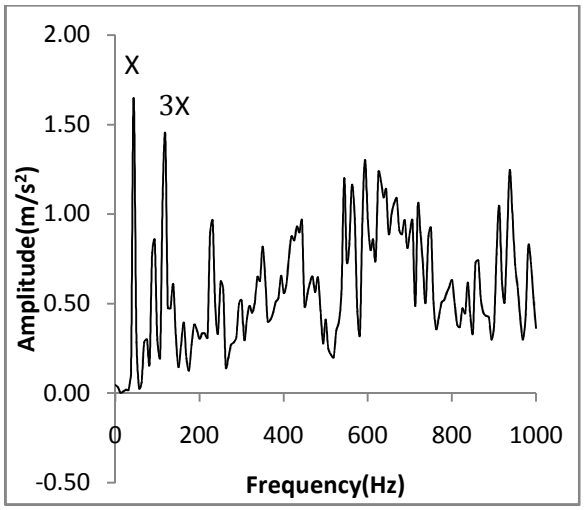

Figure 4.64 Response of transverse crack (2mm) at 2500 rpm

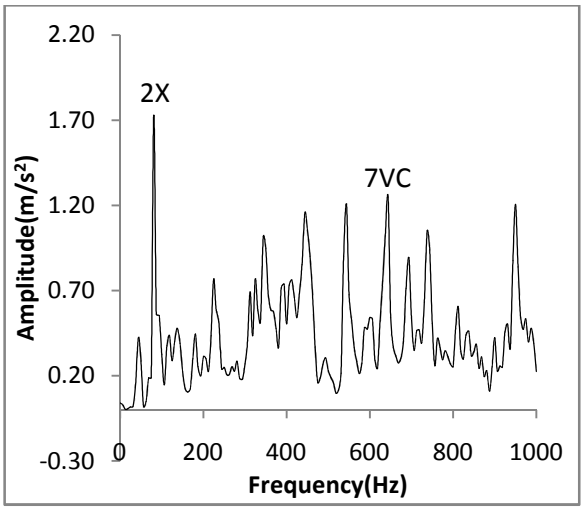

Figure 4.65 Response of slant crack (2mm) at 2500 rpm

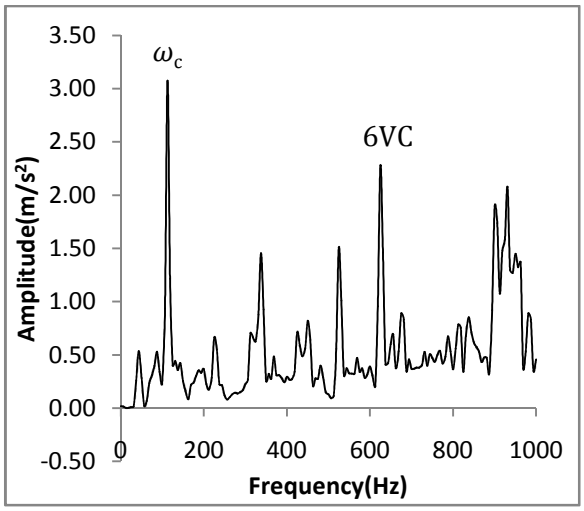

Figure 4.66 Response of transverse crack (4mm) at 2500 rpm

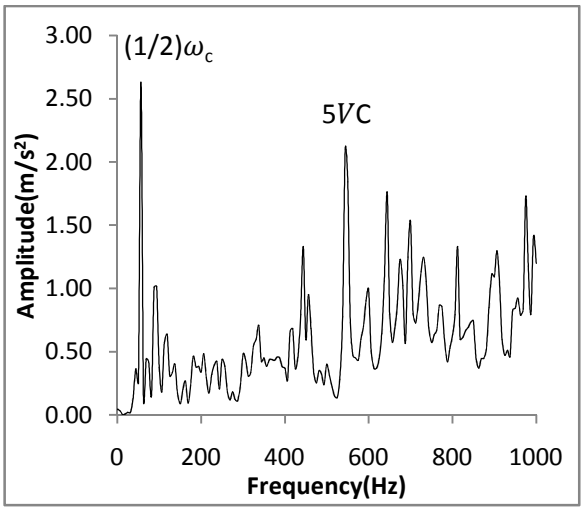

Figure 4.67 Response of slant crack (4mm) at 2500 rpm

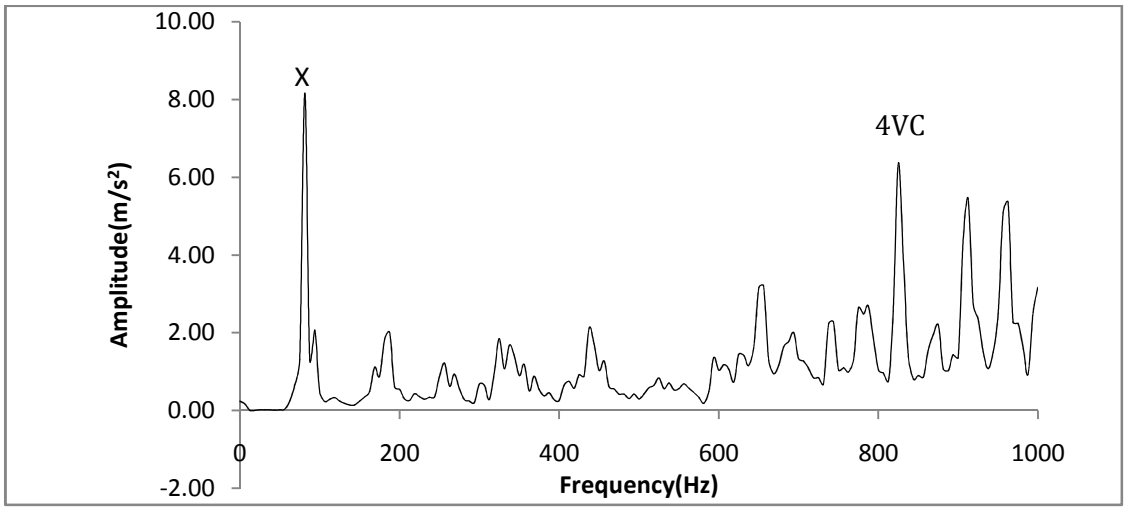

Figure 4.68 Response of healthy shaft at 5000 rpm

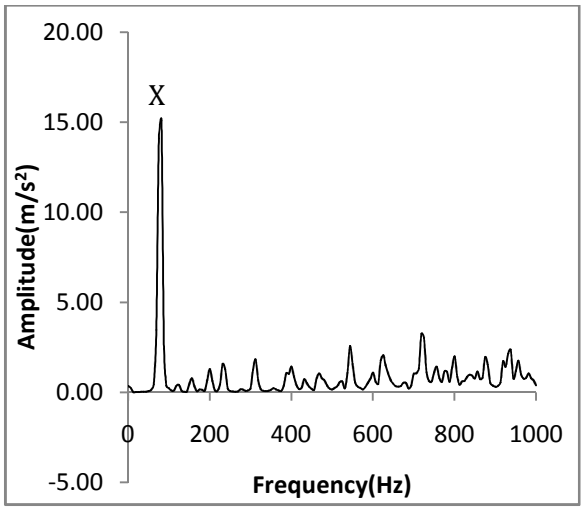

Figure 4.69 Response of bent shaft at 5000 rpm

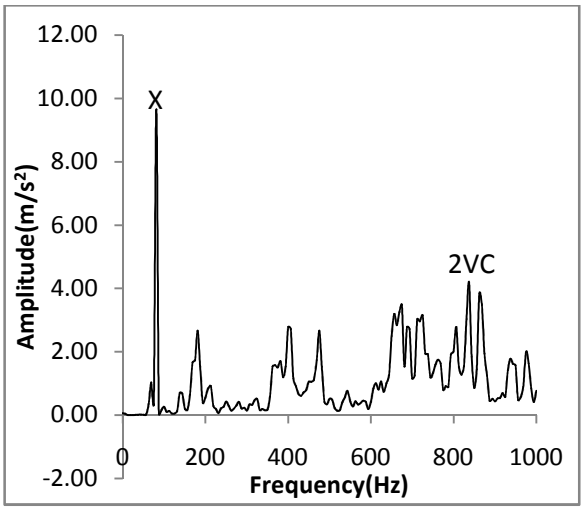

Figure 4.70 Response of misaligned shaft at 5000 rpm

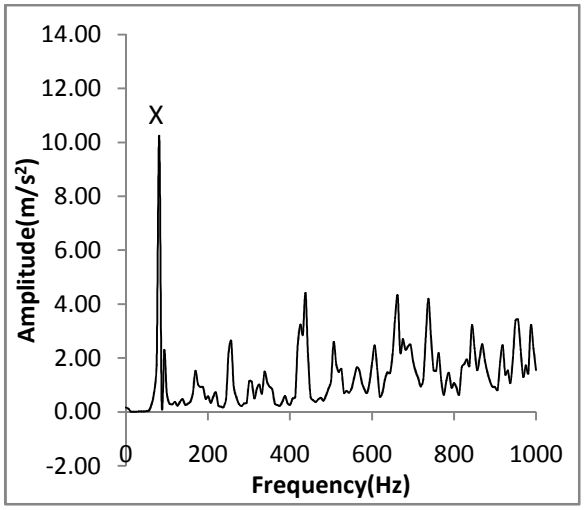

Figure 4.71 Response of transverse crack (2mm) at 5000 rpm

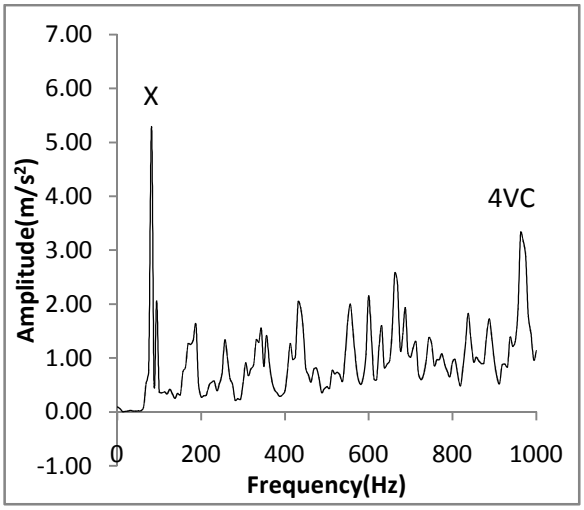

Figure 4.72 Response of slant crack (2mm) at 5000 rpm

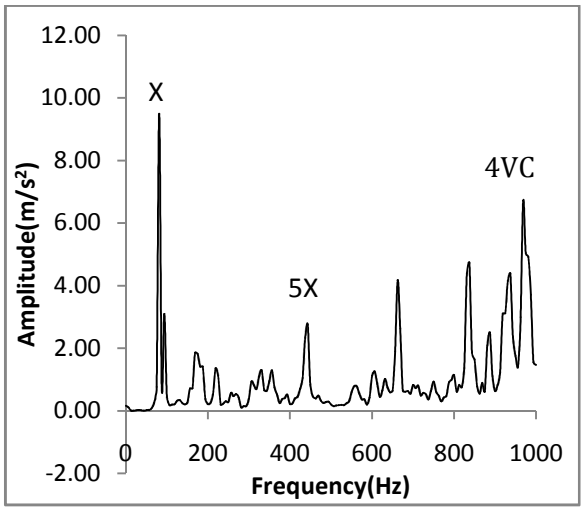

Figure 4.73 Response of transverse crack (4mm) at 5000 rpm

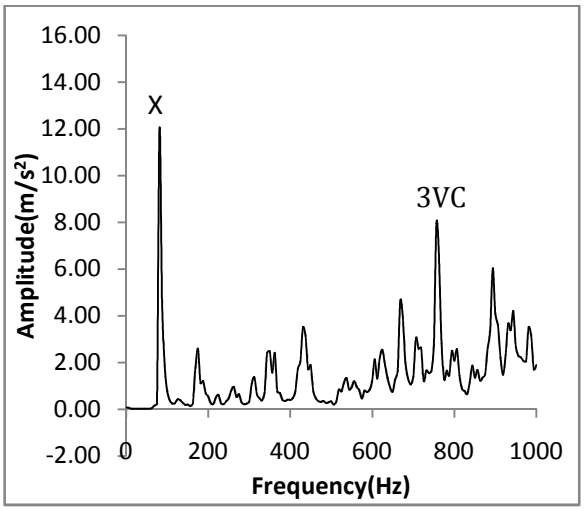

Figure 4.74 Response of slant crack (4mm) at 5000 rpm

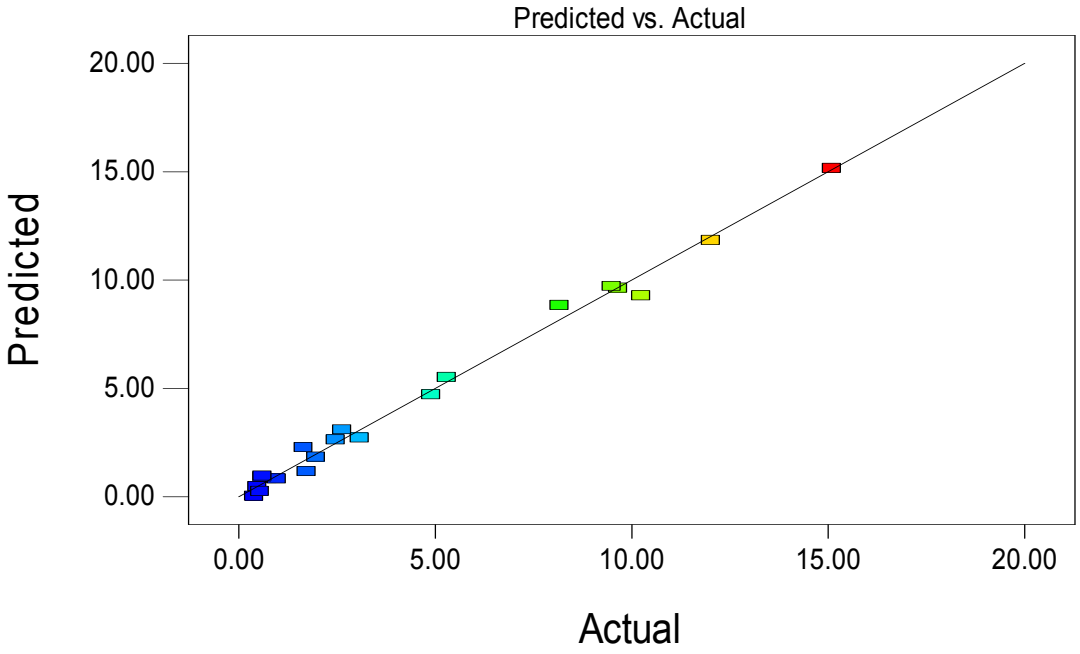

Figure 4.75 Predicted vs Actual response values

Table 4.10

Analysis of variance table for acceleration [Partial sum of squares-Type III]

Source	Sum of Squares	df	Mean Square	F Value	p-value (Prob> F)
Model	401.80	10	40.18	128.68	<0.0001
A-Bent Shaft	20.71	1	20.71	66.33	<0.0001
B-Misaligned Shaft	1.04	1	1.04	3.33	0.0982
C-Transverse Crack	1.17	1	1.17	3.74	0.0817
D-Slant Crack	4.23	1	4.23	13.55	0.0042
E-Speed	20.72	1	20.72	66.36	<0.0001
AE	12.45	1	12.45	39.86	<0.0001
DE	3.18	1	3.18	10.18	0.0097
D^2	8.20	1	8.20	26.28	0.0004
E^2	10.30	1	10.30	33.00	0.0002
D^2E	12.4	1	12.40	39.70	<0.0001
Residual	3.12	10	0.31		
Cor Total	404.92	20			

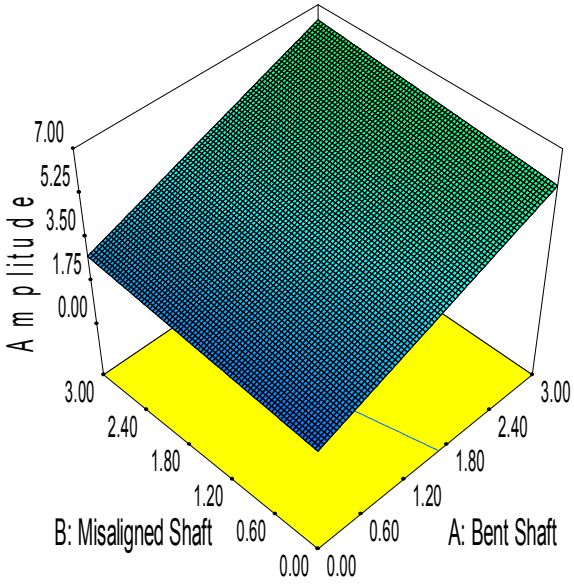

Figure 4.76 Interaction of A and B

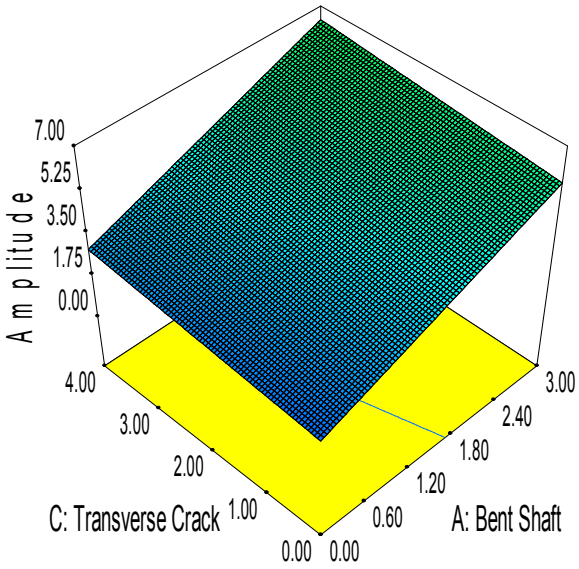

Figure 4.77 Interaction of A and C

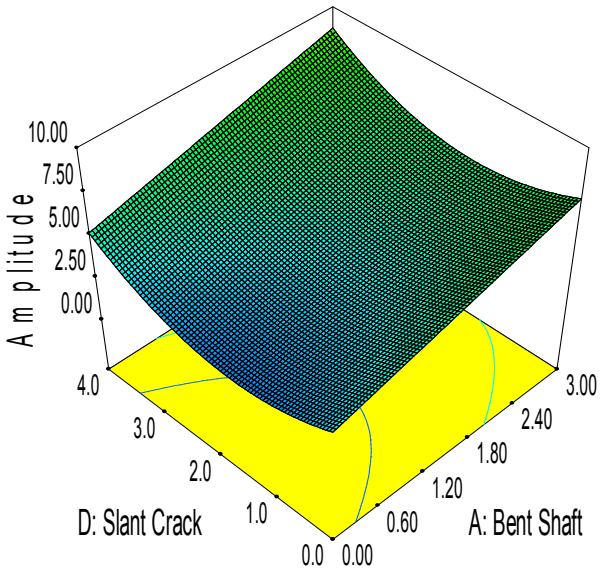

Figure 4.78 Interaction of A and D

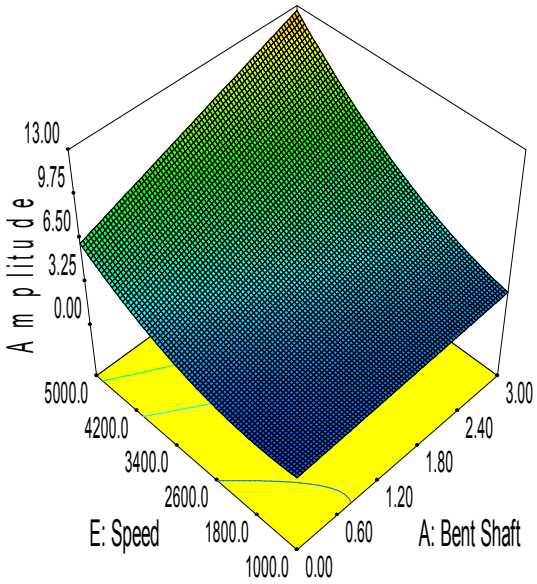

Figure 4.79 Interaction of A and E

Figures 4.76 to 4.79 show the interaction effect of bent shaft with other factors. In the above four figures it is clear that amplitude of vibration increases with the increase in the bend by keeping other factors at minimum level. In presence of bend in shaft, effect of misalignment and transverse crack is insignificant on amplitude of vibration as shown in

Figures 4.76 and 4.77. While if bend in shaft exist along with slant crack, it has significant effect on vibration amplitude as shown in Figure 4.78. Figure 4.79 shows that the amplitude of vibration also increases with increase in bend at higher rotor speed.

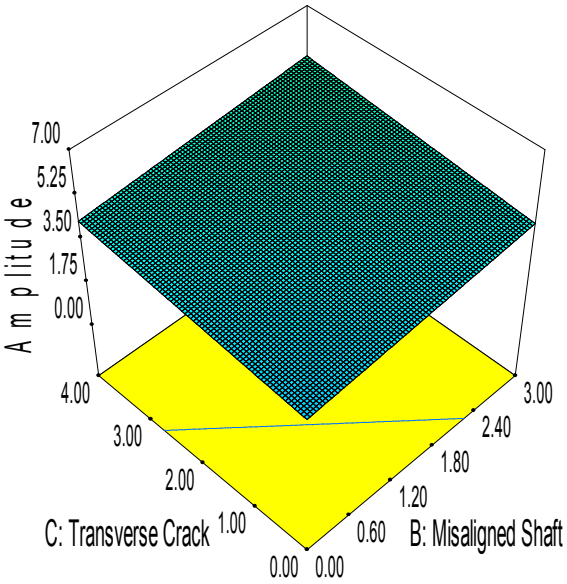

Figure 4.80 Interaction of B and C

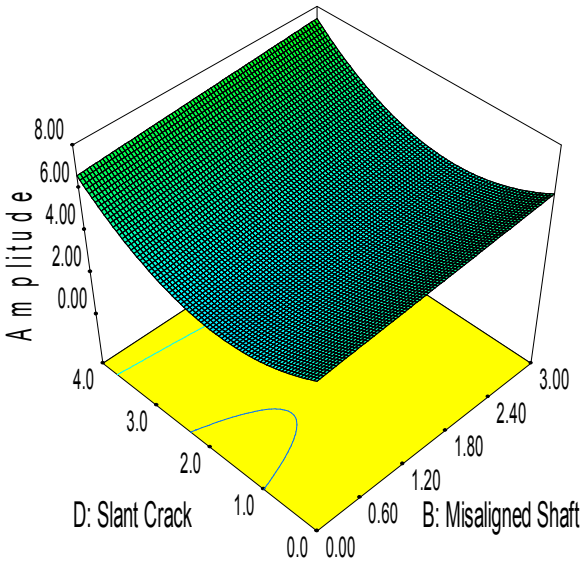

Figure 4.81 Interaction of B and D

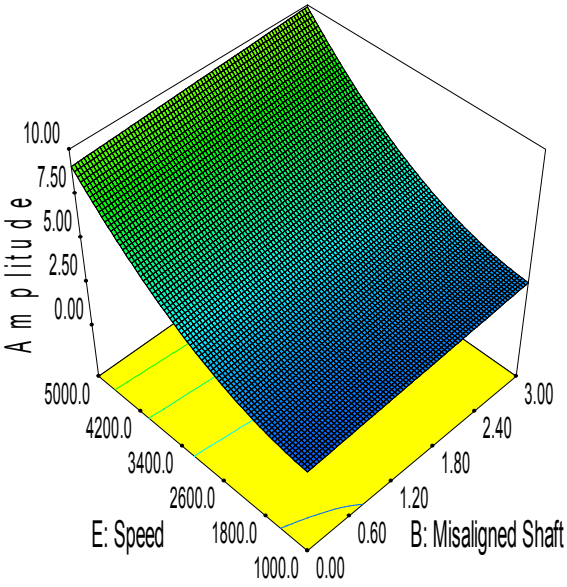

Figure 4.82 Interaction of B and E

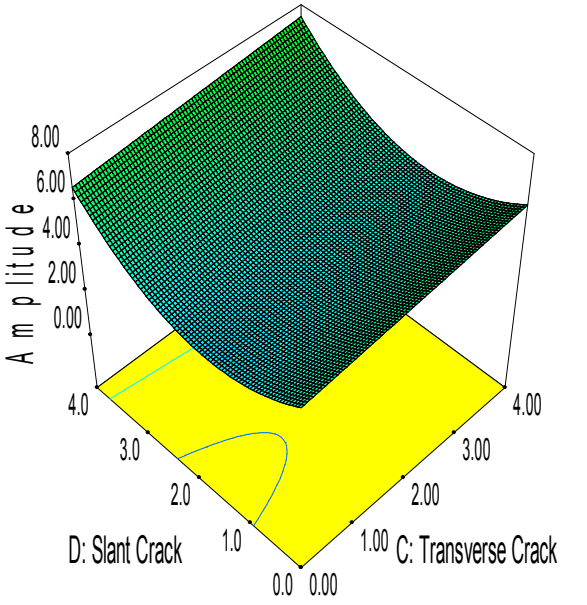

Figure 4.83 Interaction of C and D

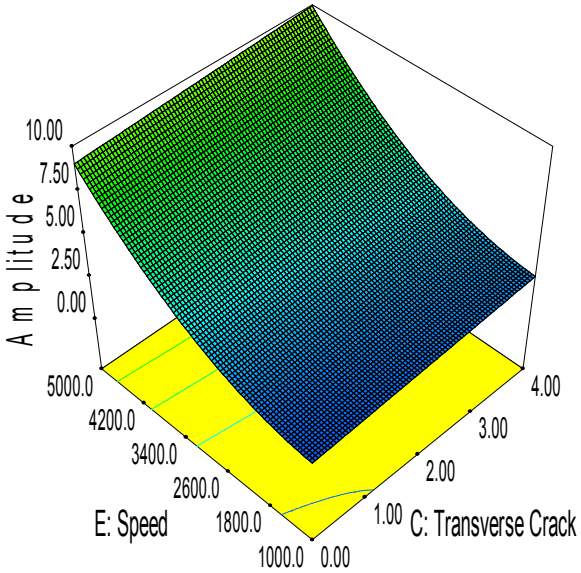

Figure 4.84 Interaction of C and E

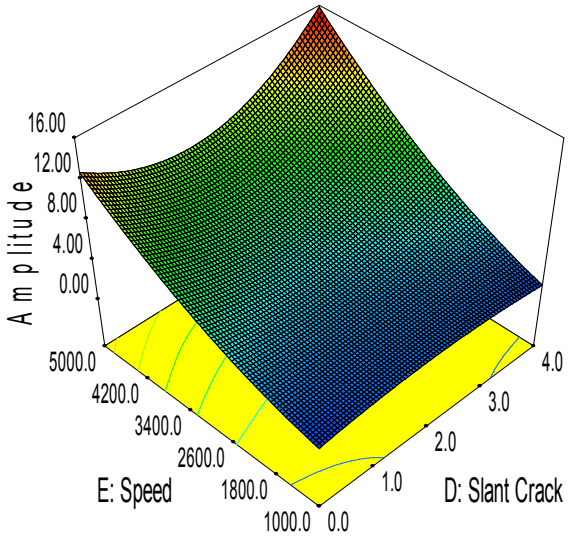

Figure 4.85 Interaction of D and E

Figure 4.80, 4.81 and 4.82 shows the interaction between misaligned shaft with transverse crack, slant crack and speed. If we take misalignment individually or interaction with transverse crack then there is very small increase in the vibration amplitude as shown in Figure 4.80. Response plot in Figure 4.81 shows the interaction of misalignment with slant crack. The vibration amplitude first increases and then decreases slightly and again increases with high amplitude. Similarly when interaction of misalignment occurs with speed (as demonstrated in Figure 4.82) then it shows large increase in vibration amplitude of the system. Figure 4.83 indicates the response surface of transverse crack and slant crack when acted together which depicts the increase in the amplitude of vibrations. Increase in amplitude of vibration in this case is mainly due to increase in severity of slant crack. Figure 4.84 shows the interaction between transverse crack and speed which expresses that vibrations increase significantly with increase in speed and transverse crack has very less effect on amplitude of vibration. Interaction of slant crack with speed is shown in the Figure 4.85, when this interaction occurs then amplitude of vibrations increases very significantly.

From Figures 4.79, 4.82, 4.84 and 4.85, it is concluded that the shaft speed is the most significant parameter which increases amplitude of vibration. Interaction of shaft speed and slant crack gives condition of severe vibration as shown in Figure 4.85. Transverse crack and misalignment has less effect on amplitude of vibration as shown in Figure 4.80.

The overall methodology for analysis using RSM is given in Figure 4.86.

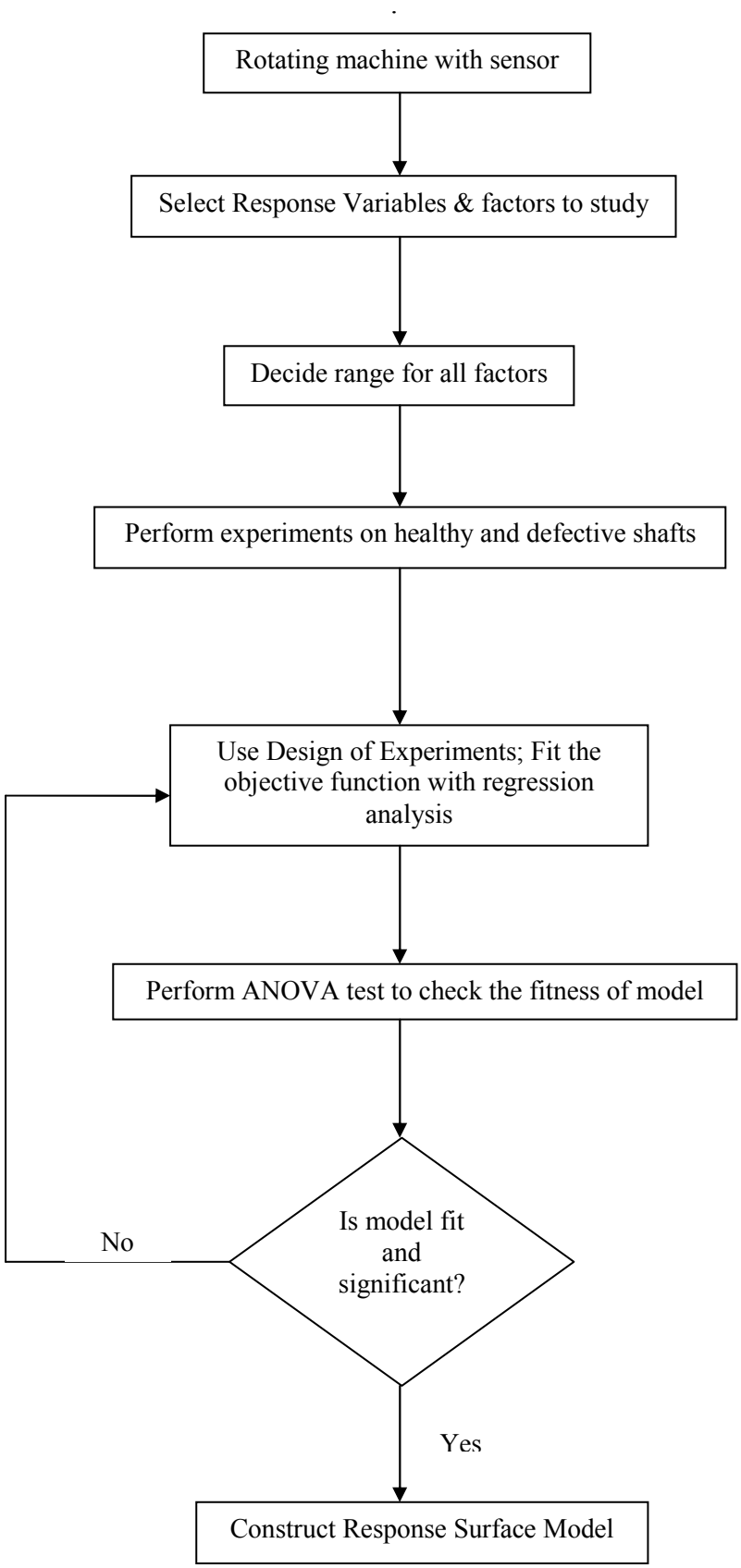

Figure 4.86 Flow Chart of RSM

Chapter 5
CONCLUSIONS

In the present study, the dynamic behaviour of a rigid healthy/defective rotor supported on healthy ball bearings is investigated. In this model, various types of defects are considered for the experimentation, these are:

1) Bent Shaft

2) Misaligned Shaft

3) Shaft having Transverse Crack (depth of 2mm, 4mm)

4) Shaft having Slant Crack at 45° (2mm, 4mm)

Due to the presence of defects in the shaft, different vibration responses are obtained in form of FFT. Results show that the every defect in shaft gives a distinguish frequency of excitation and this excitation frequency can be used to find possible causes of vibration in the rotor bearing system. Vibration responses obtained through experiments are fairly matched with theoretical frequencies of corresponding defects. Spectral analysis of response at various speeds in study, has revealed the presence of rotational frequency, sub-harmonic and super-harmonic components of critical frequency of shaft, varying compliance (*VC*) and its harmonics and linear combination of harmonics rotational frequency and varying compliance frequencies.

To study interaction between defects responses are obtained using response surface methodology (RSM). RSM provides a method to predict the vibration amplitude due to individual defects and their combination. Methodology proposed is also useful to find out significant/insignificant factors affecting amplitude of vibrations.

Following important conclusions as regards the effects of various parameters on dynamic response from the present study can be made:

5.1 EFFECT OF BEND IN SHAFT

1) For Bent shaft defect, the vibration spectrum has components mainly at rotational frequency (*X*) and at multiple of the rotational frequency.

2) In this case, the other major peaks appear at the multiple of varying compliance frequency (*VC*) and rotational frequency of shaft (*X*).

3) The amplitude of vibration increases with increase in speed of shaft.

5.2 EFFECT OF MISALIGNED SHAFT

1) In this case vibration spectra show the apex values at the multiple of rotational frequency (*X*).

2) The neighboring peak values appear on the multiple of varying compliance frequency and rotational frequency.

3) Vibration responses are gives more irregular pattern than in case of bent shaft.

5.3 EFFECT OF TRANSVERSE CRACK

1) Vibration responses of transverse crack have been obtained with depth of crack as 4mm. The spectrum shows the peak amplitudes come out at the sub-harmonic of critical frequency of shaft (ω_c) at lower speed of shaft. At higher shaft speed vibration peak appears at rotational frequency of the shaft (*X*).

2) As speed of shaft increases, amplitude of vibration also increases.

5.4 EFFECT OF SLANT CRACK

1) Experimentation in the case of slant crack is done at crack depth 4mm at the angle of 45°. The response shows that the main peak amplitude occurs at either on half of critical frequency ($(1/2)\omega_c$) or rotational frequency(*X*).

2) The neighboring frequencies are on multiple of varying compliance frequency (*VC*) or critical frequency.

3) In case of slant crack the amplitudes are lesser than that in transverse crack.

5.5 INTERACTIVE EFFECT OF DEFECTS USING RESPONSE SURFACE METHODOLOGY (RSM)

In this investigation, response surface methodology (RSM) procedures are used to conduct number of tests for investigating co-occurring effect of defects with three level of each factors including rotor speed. From the observed responses, the following conclusions are drawn:

1) Maximum vibration occurs when the interaction of the defects takes place with speed

of the rotor and speed of shaft is found as a most significant factor affecting vibration amplitudes.

2) Interaction of shaft speed and slant crack gives condition of severe vibration. The highest amplitude of vibration acceleration is observed in the case when slant crack of 4mm interacts with the speed at 5000 rpm.

3) There is not much increase in the amplitude when misalignment and transverse crack occur simultaneously. So, misalignment and transverse cracks are the least significant factors affecting vibration amplitude.

The current study gives designers a diagnostic tool for predicting the trends of instability in a rotor bearing system for healthy and defective shaft conditions. The devised tool has capability of quantifying the amplitude of vibration based on severity of defects in shafts. In such cases, severe vibration has occurred in the system only due to either large slant crack or due to high level of shaft speed. Hence, a design/maintenance engineer can directly treat the problem just using information from vibration spectra. With the features available in the devised diagnostic tool, the proposed model can be used for design, predictive maintenance of a rotor bearing system and also for condition monitoring of high speed rotating machines.

5.6 SCOPE FOR FUTURE WORK

Although a lot of work has been done in the area of fault diagnosis, still there exists a gap in literature to study the effect of defect severity and multiple types of defects on vibration response of the system. More investigations are related to the diagnosis and prognosis of bearing and rotor faults of dynamic nature can be analyzed. Integrate the diagnostic techniques developed for the bearings, gears, shafts, and power transmission components with the proposed scheme to create a comprehensive monitoring system for high speed rotary machinery.

REFERENCES

1. Babu T. R, Sekhar A.S, Detection of two cracks in a rotor-bearing system using amplitude deviation curve, Journal of Sound and Vibration, Vol. 314, 2008, pp. 457–464.
2. Bachschmid N, Pennacchi P, Tanzi E, A sensitivity analysis of vibrations in cracked turbo generator units versus crack position and depth, Mechanical Systems and Signal Processing, Vol. 24, 2010, pp. 844–859.
3. Bachschmid N, Tanzi E, Audebert S, The effect of helicoidal cracks on the behaviour of rotating shafts, Engineering Fracture Mechanics 75, 2008, 475–488.
4. Box, G.E.P. and Wilson, K.B., On the experimental attainment of optimum conditions, Journal of Royal. Statistical Society, Series B, Vol. 13 (1), 1951, pp. 1-35.
5. Chan R. K. C and Lai T. C, Digital simulation of rotating shaft with transverse crack, Vol. 19, 1995, pp. 411-420.
6. Chasalevris A.C, Papadopoulos C.A, A continuous model approach for cross-coupled bending vibrations of a rotor-bearing system with a transverse breathing crack, Mechanism and Machine Theory Vol. 44, 2009, pp. 1176–1191.
7. Cheng L, Li N, Chen X-F, He Zheng-Jia, The influence of crack breathing and imbalance orientation angle on the characteristics of the critical speed of a cracked rotor, Journal of Sound and Vibration, Vol. 330, 2011, pp. 2031–2048.
8. CNC Router, http://www.cncroutersource.com/leadscrew.html, 2007
9. Darpe A. K, Gupta K and Chawla A, Dynamics of a two-crack rotor, Journal of Sound and Vibration, Vol. 259(3), 2003 (a), pp. 649–675.
10. Darpe A.K, Gupta K, Chawla A, Experimental investigations of the response of a cracked rotor to periodic axial excitation, Journal of Sound and Vibration, Vol. 260, 2003 (b), pp. 265–286.
11. Darpe A.K, Gupta K, Chawla A, Transient response and breathing behaviour of a cracked Jeffcott rotor, Journal of Sound and Vibration, Vol. 272, 2004, pp. 207–243.

12. Darpe A. K, A novel way to detect transverse surface crack in a rotating shaft, Journal of Sound and Vibration, ID 305, 2007 (a), pp. 151–171.

13. Darpe A. K, Coupled vibrations of a rotor with slant crack, Journal of Sound and Vibration, Vol. 305, 2007 (b), pp. 172–193.

14. Davies, W.G.R. and Mayes, I.W., The vibrational behaviour of a multi-shaft, multi-bearing system in the presence of a propagating transverse crack, Trans ASME J Vib Acoust Stress Reliab Des, Vol. 106, 1984, pp. 146–53.

15. Dong H. B, Chen X.F, Li B, Qi K.Y, He Z.J, Rotor crack detection based on high-precision modal parameter identification method and wavelet finite element model, Mechanical Systems and Signal Processing, Vol. 23, 2009, pp. 869–883.

16. Elforjani M, Mba D, Detecting natural crack initiation and growth in slow speed shafts with the Acoustic Emission technology, Engineering Failure Analysis, ID 16, 2009, pp. 2121–2129.

17. Freitas M, Reis L, Fonte M, Li B, Effect of steady torsion on fatigue crack initiation and propagation under rotating bending: Multiaxial fatigue and mixed-mode cracking, Engineering Fracture Mechanics, Vol. 78, 2010, pp. 826–835.

18. Gallina, A, Martowicz, A and Uhl, T, An application of response surface methodology in the field of dynamic analysis of mechanical structures considering uncertain parameters, ISMA 2006 Conference, Leuven, Belgium.

19. Han D J, Vibration analysis of periodically time-varying rotor system with transverse crack, Mechanical Systems and Signal Processing, Vol. 21, 2009, pp. 2857–2879.

20. Jasmine, http://cbm-predictive.blogspot.com/2010/08/misalignment.html, 2010

21. Kankar P. K, Fault diagnosis of rolling element bearings using vibration signature analysis, Ph.D. Thesis, Indian Institute of Technology, Roorkee, 2011.

22. Kankar P.K, Harsha S.P, Kumar P, Sharma S. C, Fault diagnosis of a rotor bearing system using response surface method, European Journal of Mechanics A/Solids, Vol. 28, 2009, pp. 841–857.

23. Khalid Y.A, Mutasher S.A, Sahari B.B, Hamouda A.M.S, Bending fatigue behavior of hybrid aluminum/composite drive shafts, Materials and Design 28, 2007, pp. 329–334.

24. Lees A.W, Misalignment in rigidly coupled rotors, Journal of Sound and Vibration, Vol. 305, 2007, pp. 261–271.

25. Liang, X., Lin, Z. and Zhu, P., Acoustic analysis of damping structure with response surface method, Applied Acoustics, Vol. 68, 2007, pp. 1036-1053.

26. Lin Y, Chu F, The dynamic behavior of a rotor system with a slant crack on the shaft, Journal of Mechanical Systems and Signal Processing, Vol 24, 2010, pp. 522–545.

27. Mania G, Quinna D.D, Kasardab M, Active health monitoring in a rotating cracked shaft using active magnetic bearings as force actuators, Journal of Sound and Vibration Vol. 294, 2006, pp. 454–465.

28. Mayes, I. and Davies, W., The vibrational behaviour of a rotating system containing a transverse crack, In: IMechE conference on vibrations in rotating machinery, Vol. C/168/76, 1976, pp. 53–64.

29. Mayes, I.W., Davies, W.G.R., Analysis of the response of a multi-rotor-bearing system containing a transverse crack in a rotor, Transactions of ASME J Vib Acoust Stress Reliab Des, Vol. 106, 1984, pp. 139–45.

30. Myers, R. H. and Montgomery, D.C., Response surface methodology: Process and product optimization using designed experiments, Wiley, New York, 1995.

31. Papadopoulos C. A, The strain energy release approach for modeling cracks in rotors: A state of the art review, Mechanical Systems and Signal Processing, ID. 22, 2008, pp. 763–789.

32. Patel T. H, Darpe A. K, Coupled bending-torsional vibration analysis of rotor with rub and crack, Journal of Sound and Vibration Vol. 326, 2009 (), pp. 740–752.

33. Patel T. H, Darpe A. K, Experimental investigations on vibration response of misaligned rotors, Mechanical Systems and Signal Processing, Vol. 23, 2009 (b), pp. 2236–2252.

34. Patel T. H, Darpe A. K, Study of coast-up vibration response for rub detection, Mechanism and Machine Theory, Vol. 44, 2009 (a), pp. 1570–1579.

35. Patel T. H, Darpe A. K, Vibration response of a cracked rotor in presence of rotor–stator rub, Journal of Sound and Vibration 317 (2008) 841–865.

36. Patel T. H, Darpe A. K, Vibration response of misaligned rotors, Journal of Sound and Vibration, Vol. 325, 2009 (c), pp. 609–628.

37. Pennacchi P, Bachschmid N, Vania A, A model-based identification method of transverse cracks in rotating shafts suitable for industrial machines, Mechanical Systems and Signal Processing, Vol. 20, 2006, pp. 2112–2147.

38. Prabhakar S, Sekhar A. S and Mohanty A. R, Detection and monitoring of cracks in a rotor-bearing system using wavelet transforms, Mechanical Systems and Signal Processing, Vol. 15(2), 2001, pp. 447-450.

39. Randall R B, A book on Vibration based condition monitoring, John Wiley and Sons, Ltd., Publication, 2011.

40. Rubio L, Munoz-A B, Loaiza G, Static behaviour of a shaft with an elliptical crack, Mechanical Systems and Signal Processing, Vol. 25, 2011, pp. 1674–1686.

41. Sabnavis G, Kirk R. G, Kasarda M and Quinn D, Crack shaft detection and diagnostics: A litreture review, The schock and vibration digest, Vol.36 (4), 2004, pp. 287-296.

42. Sekhar A.S, Mohanty A.R, Prabhakar S, Vibrations of cracked rotor system: transverse crack versus slant crack, Journal of Sound and Vibration, Vol. 279, 2005, pp. 1203–1217.

43. Sinou J-J, Detection of cracks in rotor based on the 2X and 3X super-harmonic frequency components and the crack–unbalance interactions, Communications in Nonlinear Science and Numerical Simulation, Vol. 13, 2008, pp. 2024–2040.

44. Sinou. J-J, Lees. A.W, A non-linear study of a cracked rotor, European Journal of Mechanics A/Solids, Vol. 26, 2007, pp. 152–170.

45. Sinou. J-J, Lees. A.W, The influence of cracks in rotating shafts, Journal of Sound and Vibration, Vol. 285, 2005, pp. 1015–1037.

46. Wu M-C and Huang S-C, Vibration and crack detection of a rotor with speed-dependent bearings, Vol. 40, No. 6, 1998, pp. 545—555.